© 2020. Published by The Company of Biologists Ltd | Development (2020) 147, dev186742. doi:10.1242/dev.186742

RESEARCH ARTICLE

# PRP8A and PRP8B spliceosome subunits act coordinately to control pollen tube attraction in *Arabidopsis thaliana*

**Katarína Kulichová[1,*], Vinod Kumar[1], Lenka Steinbachová[1], Božena Klodová[1], Ljudmilla Timofejeva[1], Miloslav Juříček[1], David Honys[1,2] and Said S. Hafidh[1,*,‡]**

## ABSTRACT

Precise guided pollen tube growth by the female gametophyte is a prerequisite for successful sexual reproduction in flowering plants. Cysteine-rich proteins (CRPs) secreted from the embryo sac are known pollen tube attractants perceived by pollen tube receptor-like kinases. How pre-mRNA splicing facilitates this cell-to-cell communication is not understood. Here, we report a novel function of Pre-mRNA PROCESSING factor 8 paralogs, PRP8A and PRP8B, as regulators of pollen tube attraction. Double mutant *prp8a prp8b* ovules cannot attract pollen tubes, and *prp8a prp8b* pollen tubes fail to sense the ovule's attraction signals. Only 3% of ovule-expressed genes were misregulated in *prp8a prp8b*. Combination of RNA sequencing and the MYB98/LURE1.2-YFP reporter revealed that the expression of MYB98, LUREs and 49 other CRPs were downregulated, suggesting loss of synergid cell fate. Differential exon usage and intron retention analysis revealed autoregulation of PPR8A/PRP8B splicing. *In vivo*, PRP8A co-immunoprecipitates with splicing enhancer AtSF3A1, suggesting involvement of PRP8A in 3′-splice site selection. Our data hint that the PRP8A/PRP8B module exhibits spliceosome autoregulation to facilitate pollen tube attraction via transcriptional regulation of MYB98, CRPs and LURE pollen tube attractants.

**KEY WORDS: Pre-mRNA PROCESSING factor 8, Splicing, Post-transcriptional regulation, Cell-to-cell signaling, Cysteine-rich proteins, Pollen tube attraction and reception, Sexual reproduction**

## INTRODUCTION

In flowering plants, two sperm cells are delivered to the female gametophyte for fertilization via a pollen tube after guided growth through the transmitting tract and the micropyle (Palanivelu et al., 2006; Dresselhaus and Franklin-Tong, 2013; Higashiyama and Yang, 2017). Both phases of pollen tube guidance rely on prelaid chemoattractants secreted by synergid cells and encoded by Cysteine-rich proteins (CRPs) and the Defensin-like subfamily of CRPs (DEFL) including LUREs (Márton et al., 2005, 2012; Okuda et al., 2009; Takeuchi and Higashiyama, 2012). Genes encoding the LURE family of proteins are specifically expressed in the synergid cells and their expression is under the control of MYB98 transcription factor, which is also synergid cell-specific (Kasahara et al., 2005). Intriguingly, expression of MYB98 is controlled by the central cell-specific RNA pol II component, Central Cell Guidance (CCG) and CCG Binding Protein 1 (CBP1), implying cell-to-cell pollen tube guidance control mediated by the central cell (Li et al., 2015). Pollen tube attraction and fertilization is inhibited in *ccg* and *cbp1*, suggesting an indispensable role of the central cell in pollen tube guidance (Li et al., 2015). Furthermore, several other secreted CRPs are expressed specifically from the central cell; however, their role is still unknown (Li et al., 2015). These relayed cell-to-cell signals between the two gametophytes are perceived by primary cell surface receptors at the micropyle and pollen tube tip, including female receptors such as LORELEI (Liu et al., 2016), LORELEI-LIKE GPI-anchored protein 1 (LLG1) and FERONIA, and male receptors such as COBRA GPI-anchored, MALE DISCOVERER1 (MDIS1) and MDIS2 from the LRR-VI subfamily, MDIS1-INTERACTING RECEPTOR LIKE KINASE 1 (MIK1) and MIK2 from LRR-XI and LRR-XII subfamilies, respectively, POLLEN RECEPTOR-LIKE KINASE 6 (PRK6) and palmitoylated LOSS IN POLLEN TUBE GUIDANCE 1 (LIP1) and LIP2 LURE receptors (Higashiyama and Yang, 2017). Collectively, the dominant feature of pollen tube guidance seems to rely on protein secretion and, thus, endomembrane and unconventional protein secretion mechanisms are likely to play fundamental roles in pollen tube attraction and guidance (Liu et al., 2015; Hafidh et al., 2016b).

In *Arabidopsis*, almost 90% of the genes are interrupted by introns and it is estimated that >60% of intron-containing genes undergo alternative splicing (AS) (Berget et al., 1977; Syed et al., 2012; Marquez et al., 2012; Reddy et al., 2013). Most frequently, 51% of the AS events utilize alternative 5′ or 3′ splice sites or exon skipping, influencing alternative protein coding sequences or aberrant mRNA production (McGlincy and Smith, 2008; Kalyna et al., 2012; Syed et al., 2012; Filichkin et al., 2015). Pre-mRNA splicing is mediated by the spliceosome complex, which catalyzes two sequential transesterification reactions to excise the interspaced intron (reviewed by Will and Lührmann, 2011). The spliceosome is composed of multiple subunits, the U2-dependent spliceosome type from U1, U2, U5 and U4/U6 small nuclear ribonucleoproteins (snRNPs) and numerous non-snRNP proteins. A few proteins remain as core components of the tri-snRNP complex, including Snu114, Brr2 and PRP8. PRP8A interacts with a preformed U4/U6.U5 tri-snRNP complex to form a larger catalytically active spliceosomal B complex (Maeder et al., 2009; Bartels et al., 2002). To select an alternative splice site, splicing factors bind to exonic/intron enhancer or suppressor sequence elements to influence recruitment of the spliceosome complex, resulting in alternative splicing (Staiger and Brown, 2013). Genetic screen of AtSF3A1a-U2-associated *ATROPOS* (Moll et al., 2008), U4/U6-associated LACHESIS (Gross-Hardt et al., 2007) and U5-associated

[1]Institute of Experimental Botany of the Czech Academy of Sciences, Rozvojová 263, 165 02 Prague 6, Czech Republic. [2]Department of Plant Experimental Biology, Faculty of Science, Charles University, Viničná 5, 128 44 Prague 2, Czech Republic. *These authors contributed equally to this work

‡Author for correspondence (hafidh@ueb.cas.cz)

K.K., 0000-0002-1115-9899; L.T., 0000-0002-1046-2001; D.H., 0000-0002-6848-4887; S.S.H., 0000-0002-3970-713X

**Handling Editor: Ykä Helariutta**
**Received 25 November 2019; Accepted 14 April 2020**

Development (2020) 147, dev186742. doi:10.1242/dev.186742

CLOTHO/GAMETOPHYTIC FACTOR 1 (Liu et al., 2009) revealed the crucial role of splicing factor proteins in the development and competence of the female gametophyte for fertilization; interestingly no effect has been reported for the male gametophyte (Tzafrir et al., 2004; Coury et al., 2007; Moll et al., 2008; Liu et al., 2009).

The *Arabidopsis* genome encodes two copies of PRP8: PRP8A (AT1G80070) and PRP8B (AT4G38780). An *abnormal suspensor* 2 (*sus2*) mutant defective in PRP8A is embryo lethal (Schwartz et al., 1994), whereas PRP8B function has not been investigated. A hypomorphic *prp8a*-6 allele was further identified to be involved in splicing of long noncoding antisense transcripts (COOLAIR) that are important for the regulation of FLOWERING LOCUS C activity and could complement the *prmt5* mutant of the NineTeen complex (NTC)/Prp19, a subcomplex of the spliceosome machinery (Marquardt et al., 2014; Deng et al., 2016).

Here, we report for the first time that double mutant *prp8a prp8b* has no striking female or male gametogenesis defects, but *prp8a prp8b* specifically impairs ovule competence for pollen tube attraction and the competence of the pollen tubes to navigate towards ovules. We propose that PRP8A/PRP8B associates with AtSF3A1 and functions in defining the competence of both gametophytes to facilitate female–male communication.

## RESULTS

### PRP8B is preferentially expressed in pollen

PRP8 is well conserved in all domains of life, including all land plants (Fig. 1A). In plants, the role of pre-mRNA splicing factor PRP8A in male or female gametophytes is unknown. Moreover, the role of PRP8B, a close paralog of PRP8A, has yet to be characterized (Fig. 1A). PRP8A shows 93% identity with PRP8B; however, they exhibit polymorphisms at the N-terminal PROCN domain and the C-terminal JAB domain, as predicted by PFAM (http://pfam.xfam.org) and InterProScan (https://www.ebi.ac.uk/interpro) EMBL-EBI databases (Fig. 1B). We initially identified PRP8A as a gene whose transcripts are mostly stored in tobacco pollen tubes as late as 24 h after pollen germination, and thus we hypothesized that they probably have a late function during pollen tube growth (Hafidh et al., 2018). Comparison of publicly deposited expression datasets (Zimmermann et al., 2004; Honys and Twell, 2004; Winter et al., 2007; Borges et al., 2008; Qin et al., 2009; Loraine et al., 2013) revealed over 30-fold elevated expression of PRP8B in pollen and semi-*in vivo* pollen tubes compared with PRP8A (Fig. 1C; Fig. S1A), whereas PRP8A dominates the expression during embryogenesis and seed development (Fig. S1A) (Belmonte et al., 2013). Real time RT-qPCR verified PRP8B dominant expression in pollen and a broader expression of PRP8A (Fig. 1D). In the embryo sac, both genes were classified as expressed in synergid cells, the egg cell and the central cell (Wuest et al., 2010). In agreement with public expression datasets, RT-qPCR verified negligible expression of PRP8B at the post-globular stage of embryo development relative to PRP8A (Fig. 1D).

To investigate localization of both subunits, we constructed PRP8Apro-PRP8A::GFP and PRP8Bpro-PRP8B::GFP and monitored their localization. Signal of PRP8A-GFP was detected in the nuclei of all female gametic cells and cells of the integuments in mature ovules, whereas PRP8B could only be reliably detected in the egg and the central cell of mature ovules (Fig. 1E). In the male gametophyte, both subunits localized in sperm cells and vegetative cell nuclei of pollen and pollen tubes; however, PRP8B was only reliably detected in hydrated pollen grains and we frequently observed vegetative cytosolic localization of PRP8B (Fig. 1E). Post-

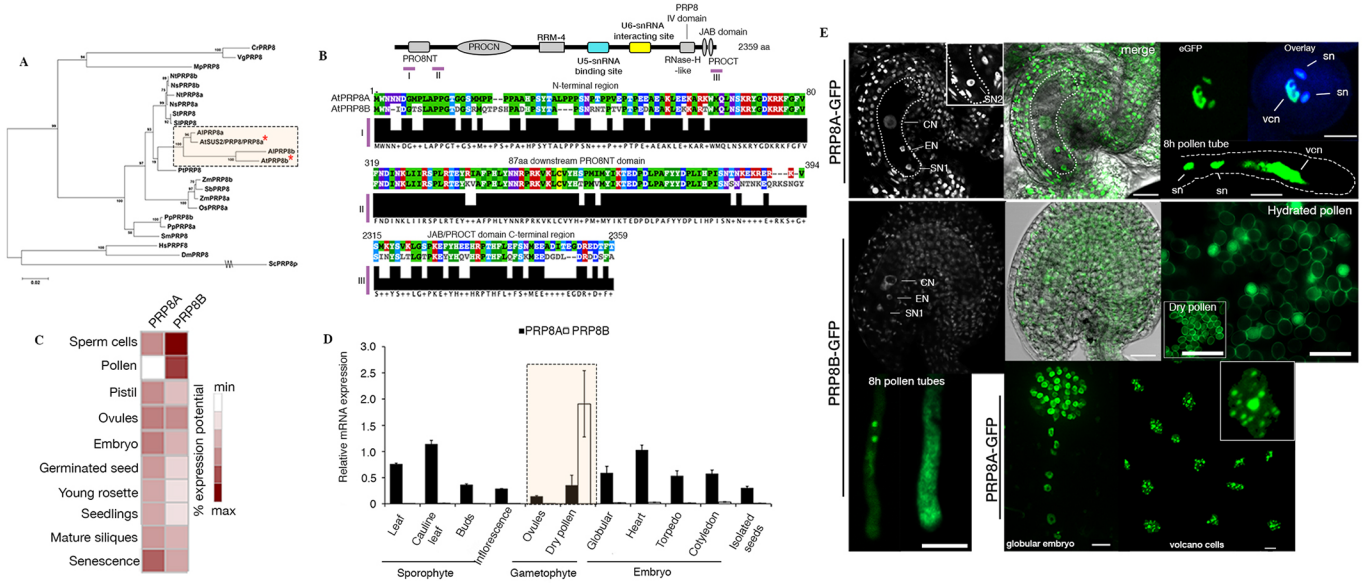


**Fig. 1. PRP8B expression is dominant in pollen and in sperm cells.** (A) Phylogeny of PRP8 orthologs in Archea, fungi, plants and animals. Asterisks indicate the two *Arabidopsis thaliana* paralogs. The scale bar indicates the rates of substitutions/site. (B) PRP8A and PRP8B are 93% identical but show polymorphisms at the PROCN and JAB domain regions. Alignment was performed with Clustal Omega and visualized with Jalview. (C) Comparative expression of *PRP8A* and *PPR8B*. Data were retrieved from Genevestigator (Zimmermann et al., 2004). This figure is extended to Fig. S1. (D) RT-qPCR verification of *PRP8A* and *PRP8B* steady-state transcript levels. Ct values of eIF4A1 were used as reference to compute relative expression. Data are mean±s.d. (E) Subcellular localization of PRP8Apro-PRP8A::GFP and PRP8Bpro-PRP8B::GFP in ovules, pollen, pollen tubes and developing globular stage embryo. Unlike PRP8A, PRP8B was not reliably detected in dry pollen and in addition to nuclear localization in pollen tubes, it also localized in the pollen tube cytoplasm. In mature ovules, PRP8B was only reliably detected in the central cell nucleus. Note the punctate subnuclear domains formed by PRP8A in epidermal cells of the seed with volcano-shaped columellae showing two distinct subpopulations. Dotted white lines highlight dominant expression of PRP8B in pollen. CN, central cell nucleus; EN, egg cell nucleus; sn, sperm cell nucleus; SN1/2, synergid cell 1 and 2 nuclei; vcn, vegetative cell nucleus. Scale bars: 40 µm.

Development (2020) 147, dev186742. doi:10.1242/dev.186742

fertilization, PRP8A localized in nuclei of developing embryo and suspensor cells and in heterogeneous nuclear speckles in volcano cells of mature seeds, whereas PRP8B was not reliably detectable.

### Double mutant *prp8a prp8b* is female and male sterile

To assess PRP8A and PRP8B function, we characterized three transfer DNA (T-DNA) insertion alleles that disrupt the U6-snRNP interacting domain of PRP8A and PRP8B, designated *prp8a*-12, *prp8a*-13 and *prp8b*-1 (Fig. 2A). Two other *PRP8B* alleles, *prp8b*-2 and *prp8b*-3, were also screened (Fig. 2A). *prp8a*-12 is embryo lethal as previously reported from other *prp8a* alleles (Schwartz et al., 1994; Tzafrir et al., 2004; Meinke et al., 2008; Marquardt et al., 2014; Deng et al., 2016); therefore, heterozygous *PRP8Aa*-12 and homozygous *prp8bb*-1 plants were selected for further characterization. Henceforth, *prp8a*-12 and *prp8b*-1 mutant alleles will be referred to as *prp8a* and *prp8b*, respectively. RT-qPCR revealed that both *prp8a* and *prp8b* are knockdown alleles (Fig. 2B). Screen of heterozygous *PRP8Aa* and homozygous *prp8bb* mutant plants showed no developmental or gametophyte abnormalities, defects in pollen tube growth, gamete cell fate specification or any reduction in transmission of the mutant alleles ($\chi^2$ test=1.53, 0.53; $P$>0.22) (Fig. S1B,C). Segregation of self-pollinated *PRP8Aa* plants confirmed the recessive homozygous embryo lethality of the *prp8a* allele (Fig. S1D). Our results implied a functional redundancy between PRP8A and PRP8B in both gametophytes. We therefore generated double mutant *prp8a prp8b* and investigated developmental phenotypic defects. No sporophytic defects could be observed throughout plant development (Fig. 2C). Instead, analysis of *PRP8Aa;Bb* and *PRP8Aa;bb* plants revealed that segregation and transmission of *prp8a prp8b* double mutant alleles was severely reduced through both the female and male gametophytes (female transmission efficiency 2.02%, male transmission efficiency 1.04%; $P$<0.001) (Fig. 2D,E). Rarely, in <4% of the cases in self-fertilized plants, *prp8a prp8b* alleles could be transmitted by either male or female gametophytes from the *PRP8Aa;bb* genotype plants (Fig. 2D). These results imply that the *prp8a prp8b* genotype is lethal in the gametophyte. In support, dissection of *PRP8Aa;bb* siliques revealed approximately 46% of unfertilized ovules ($n$=422/502) (Fig. 2F). To confirm the origin of this phenotype, we complemented *PRP8Aa;bb* plants with *PRP8A*pro-*PRP8A*-3UTR and *PRP8B*pro-*PRP8B*::*GFP* constructs. Both constructs fully complemented the unfertilized ovule phenotype, with the *PRP8*Apro-*PRP8A*-3UTR construct showing better complementation efficiency (Fig. 2F,G). Collectively, our results imply that PRP8A and PRP8B function redundantly in the gametophyte, and that PRP8A/PRP8B dual activities are essential for successful fertilization.

### PRP8A and PRP8B act redundantly to control pollen tube attraction

The full penetrance of the *prp8a prp8b* aborted ovule phenotype suggested the possibility of a defect in pollen tube attraction, reception or fertilization. To investigate, we analyzed pollen tube attractiveness, receptivity and fertilization events in *prp8a prp8b* ovules *in vivo* using live cell imaging by pollinating *PRP8Aa;bb* pistils with pollen grains expressing double markers for vegetative and sperm cells (LAT52pro::GFP;HTR10pro-HTR10::RFP), respectively. Approximately 8 h after pollination (8 HAP), we observed accurate pollen tube attraction to the micropyle, pollen tube discharge and sperm cell release in approximately 81% ($n$=228/282) of ovules when wild-type pistils of *ms1* plants were pollinated with the double marker-expressing pollen grains (Fig. 3A). When *PRP8Aa;bb* pistils were pollinated with the same double marker pollen grains, only 49% ($n$=194/400) of the ovules were successfully targeted, referring to the *PRP8A;b* heterozygous ovule genotype (Fig. 3A). In contrast, 44% ($n$=175/400) of the adjacent *prp8a prp8b* double homozygous mutant ovules were defective in pollen tube attraction or no pollen tubes approached proximity to the ovules (Fig. 3A). Rarely, we noticed single or multiple pollen tube (polytubey) attraction by the *prp8a prp8b* ovules at the micropyle, but without detectable GFP discharge, suggesting a failure in correct pollen tube attraction or reception (Fig. 3A). Polytubey attraction into a single ovule results from pollen tube reception failure (Beale et al., 2012), thus supporting our observation on the lack of *prp8a prp8b* successful pollen tube reception. This was independently verified by the lack of female or male transmission of the *prp8a prp8b* genotype as well as by segregation distortion in the F2 siblings from *PRP8Aa;bb* selfing plants (Fig. 2E).

To test the pollen tube attraction defect of *prp8a prp8b* ovules independently, we stained callose of *in vivo* pollen tubes with aniline blue in self-pollinated *PRP8Aa;bb* plants or in an outcross of *PRP8Aa;bb* female pollinated with wild-type Col-0 pollen grains at 18 HAP to further emphasize the ovule phenotype of the *prp8a prp8b* double mutant (Fig. 3B). Almost 50% ($n$=276/541) of the ovules in *PRP8Aa;bb* pistils either failed in pollen tube attraction to the micropyle entry or no pollen tubes appeared near the mutant ovule micropyle entry in self-pollinated or in an outcross experiment (Fig. 3B). We classified the ovule phenotypes into four subtypes: type I, wild type-like ovule (*PRP8A;b*) with normal pollen tube reception; type II, double mutant *prp8a;b* ovule with normal pollen tube reception; type III, ovule with no pollen tubes nearby; and type IV, ovules with pollen tubes nearby but failed to attract pollen tubes into the micropyle (i.e. attraction defect) (Fig. 3B). In the progeny of *PRP8Aa;bb* self-pollinated plants, 39% were identified as type I, 8% as type II, 27% as type III ovules and 26% as type IV (Fig. 3B; Movies 1 and 2). In the progeny of *PRP8Aa;bb*×wild type crosses, 45% were type I, 6% were type II, 31% were type III ovules and 18% were type IV (Fig. 3B; Movies 1 and 2).

The *prp8a*-12 allele is a blue-SAIL T-DNA insertion containing a LAT52pro-GUS transgene that co-segregates with the T-DNA insertion of the mutant allele. We therefore took advantage and performed a blue dot histochemical assay (Palanivelu et al., 2006), by pollinating wild-type *ms*1 pistils and *PRP8Aa;bb* pistils with wild-type pollen grains or with pollen grains expressing LAT52pro-GUS (Fig. S2). Since *LAT52* promoter activity should be restricted to pollen only (Twell et al., 1990, 1991), we observed ectopic GUS staining in the *prp8a prp8b* embryo sac before fertilization that we did not observe in control plants (Fig. S2). However, this ectopic staining was distinguishable from GUS staining of ovules targeted with pollen tubes expressing LAT52pro-GUS (Fig. S2). Therefore, we proceeded with quantification by distinguishing the two populations in *PRP8Aa;bb* pistils. Quantification of targeted ovules supported our previous results that *prp8a prp8b* ovules fail in pollen tube attraction (Fig. S2). Collectively, our results suggest that simultaneous loss of *PRP8A* and *PRP8B* severely impairs pollen tube attraction, long-distance pollen tube guidance and fertilization in *Arabidopsis*.

### PRP8A/PRP8B function is essential for pollen tube response to female attraction signals

The near-complete block of *prp8a prp8b* transmission through the male also hinted at a role of PRP8A/PRP8B in pollen tubes.

Development (2020) 147, dev186742. doi:10.1242/dev.186742

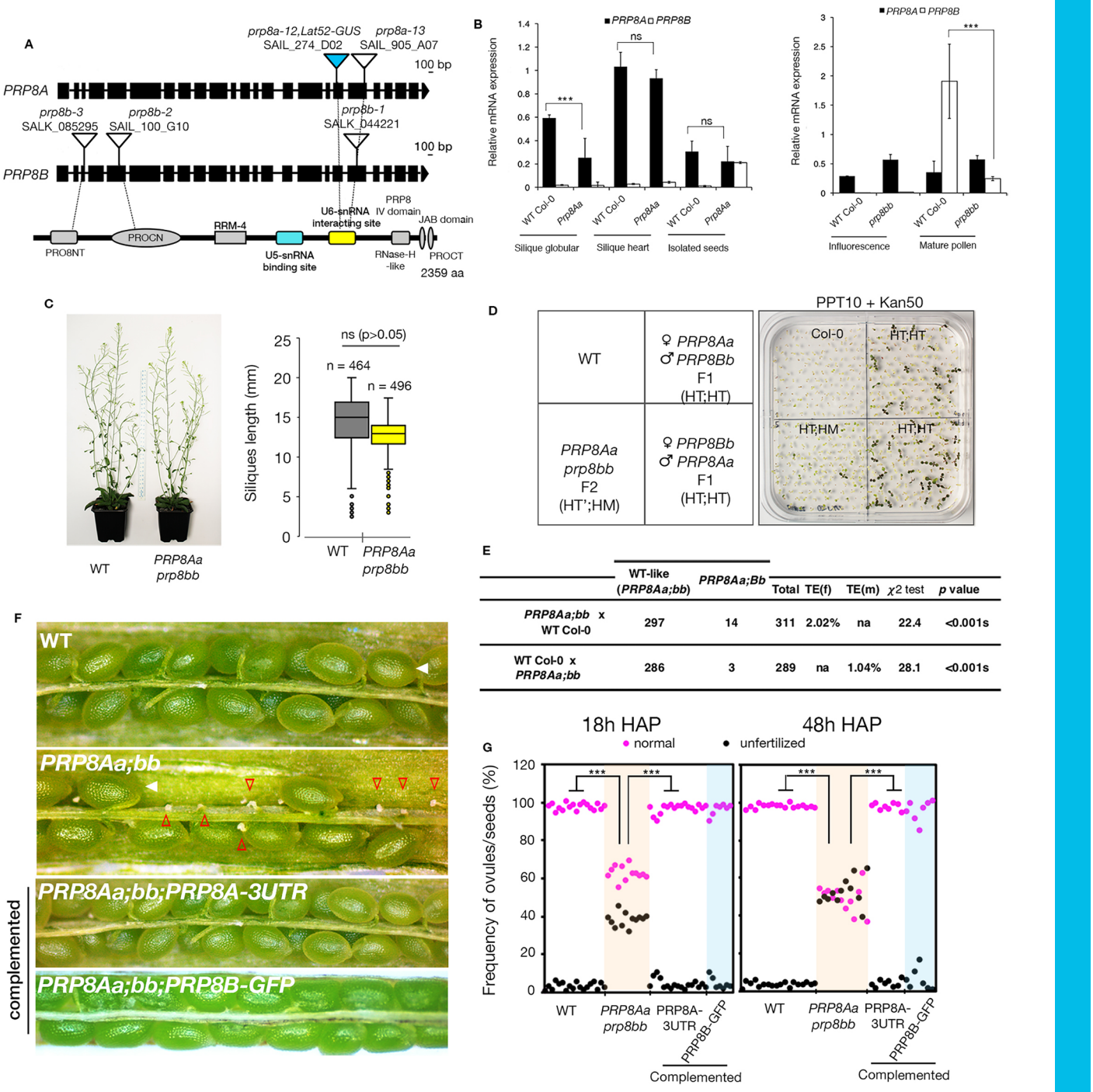


| | WT-like (*PRP8Aa;bb*) | *PRP8Aa;Bb* | Total | TE(f) | TE(m) | $\chi$2 test | *p* value |
|---|---|---|---|---|---|---|---|
| ***PRP8Aa;bb*** x **WT Col-0** | 297 | 14 | 311 | 2.02% | na | 22.4 | <0.001s |
| **WT Col-0** x ***PRP8Aa;bb*** | 286 | 3 | 289 | na | 1.04% | 28.1 | <0.001s |

**Fig. 2. Characterization of *prp8a*-12 *prp8b*-1 double mutant.** (A) Schematic of *AtPRP8a* and *AtPRP8b* loci to scale with approximate positions of the T-DNA alleles, including the blue-sail SAIL allele analyzed. Dashed lines point to protein domains disrupted by the T-DNA insertion. Lower part is the scaled protein model with domains annotated according to PFAM and PROSITE databases. (B) RT-qPCR validation of *prp8a*-12 and *prp8b*-1 knockdown alleles. Relative expression between wild-type and mutant samples was determined by normalizing the Ct values with eIF4A1 as a reference. (C) Representative images of adult wild-type and *PRP8Aa;bb* plants and siliques showing normal sporophytic development. (D,E) Segregation and transmission of the *prp8a prp8b* mutant gametes through male and female. Seedlings from selfed *PRP8Aa;bb* plants were grown under double selection (Basta, *prp8a*-12; Kan50, prp8b-1) and genotypes of resistant seedlings were verified by PCR genotyping. Transmission data for the individual alleles are in Fig. S1. TE(f) female transmission efficiency; TE(m) male transmission efficiency. (F) Dissected siliques from wild-type and *PRP8Aa;bb* plants. Triangles with red borders indicate unfertilized ovules, white triangles indicate aborted seed development and filled white triangles mark fully developed wild-type seeds. (G) Quantification of ovule phenotype in *PRP8Aa;bb* plants at 18 and 48 HAP. Complementation was performed with PRP8A-3′UTR and PRP8B-GFP under their native promoters. Data are mean±s.d. (*n*=18). ns, not significant; ***$P$<0.01 (Student's *t*-test).

Viability testing and nuclear staining revealed that *prp8a prp8b* pollen grains are viable and morphologically normal. We then exploited the LAT52pro-GUS tagged T-DNA insertion of the *prp8a*-12 SAIL allele (Fig. 2A) to follow specifically *prp8a prp8b* mutant pollen tube growth *in vitro* as well as within the pistil by GUS staining. GUS staining revealed that *in vitro prp8a prp8b*

Development (2020) 147, dev186742. doi:10.1242/dev.186742

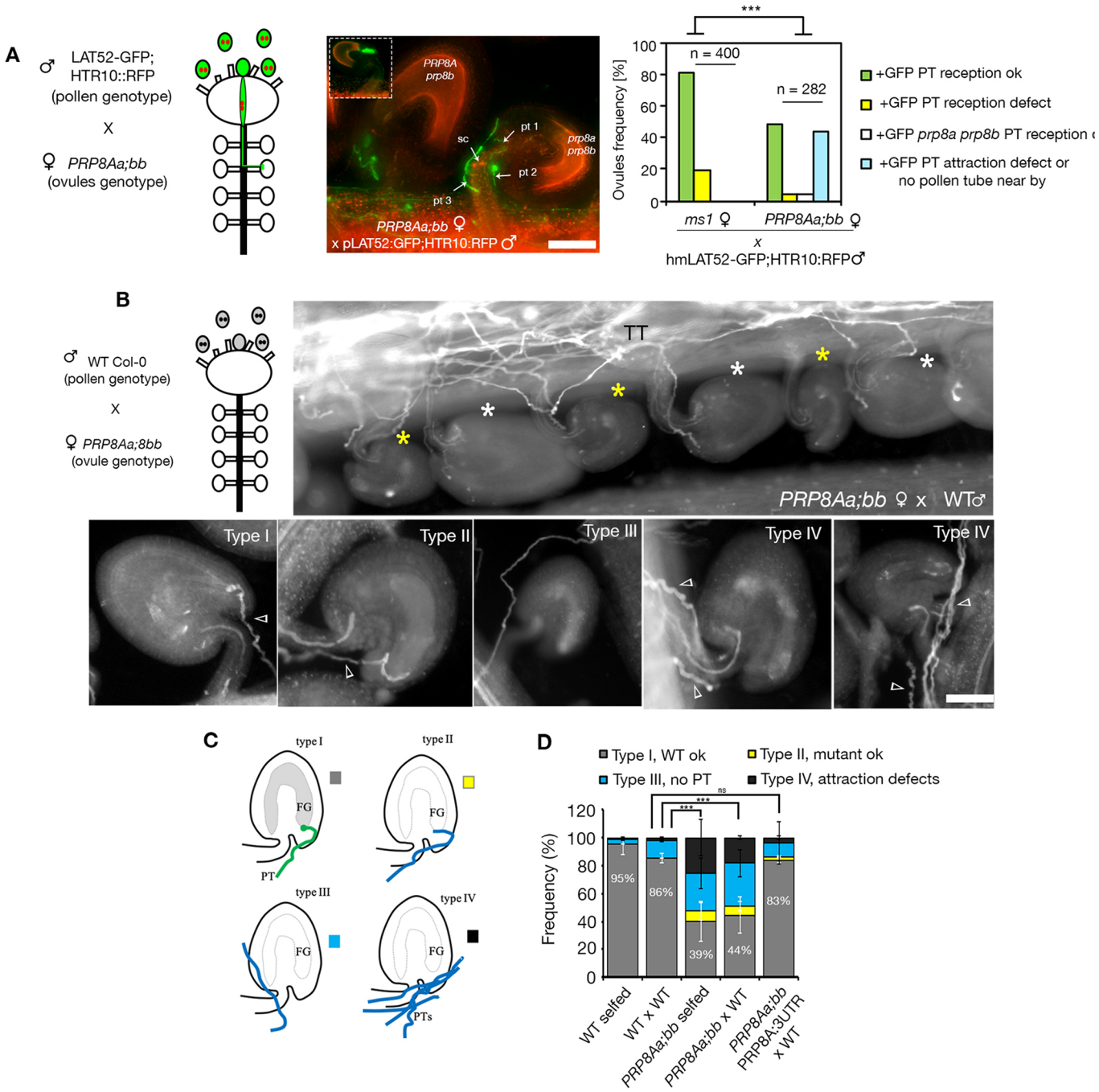


**Fig. 3. PRP8A/PRP8B controls ovule competence for pollen tube attraction.** (A) Live cell imaging of *prp8a prp8b* ovule fertilization using a dual pollen tube reporter. LAT52pro::GFP labeled the pollen tube cytosol and pHTR10-HTR10::RFP labeled sperm cells nuclei. Left ovule is wild-type-like (*PRP8A;8b* genotype), showing attraction and reception of pollen tube indicated by the GFP halo in the inset. On the right is a representative double mutant *prp8a prp8b* ovule showing attraction and a rare reception defect of multiple pollen tubes at 18 HAP. Bar chart is a quantification of ovule attraction efficiency of the respective genotypes crosses. Pt, pollen tube; sc, sperm cells. (B) *In vivo* quantification of *PRP8a;8b* pollen tube attraction defect. Top panel shows behavior of both genotypes *PRP8A;8b* (white asterisks) and *prp8a prp8b* (yellow asterisks) on pollen tube attraction and reception. Bottom panels show representative pictographs of type I-IV ovules. Type I-II, correct pollen tube reception; type III, no pollen tube within approximately 100 µm of the ovule; type IV, attraction defect (pollen tube nearby but failed to enter the micropyle). Triangles point to pollen tubes. TT, transmitting track. (C) Illustration of the *prp8a prp8b* ovules pollen tube attraction phenotype. (D) Frequency of the four types of phenotypes in each respective cross at 18 HAP. Data are mean±s.d. ns, not significant; ***$P$<0.01 (Student's $t$-test). Scale bars: 50 µm.

pollen tube growth is indistinguishable from that of wild-type pollen tubes (Fig. 4A). *In vivo*, double mutant *prp8a prp8b* pollen tube growth also appeared normal in the transmitting tract and the double mutant pollen tubes were able to reach the very bottom of the pistil, suggesting no growth or navigation defects in the transmitting tract (Fig. 4B). However, compared with control LAT52pro-GUS pollen tubes, the *prp8a prp8b* pollen tubes failed to turn towards the funiculus or target any ovules in wild-type pistils (0% targeted, $n$=0/391 ovules) (Fig. 4B). These results are in agreement with the blocked transmission of *prp8a prp8b* alleles through the male

Development (2020) 147, dev186742. doi:10.1242/dev.186742

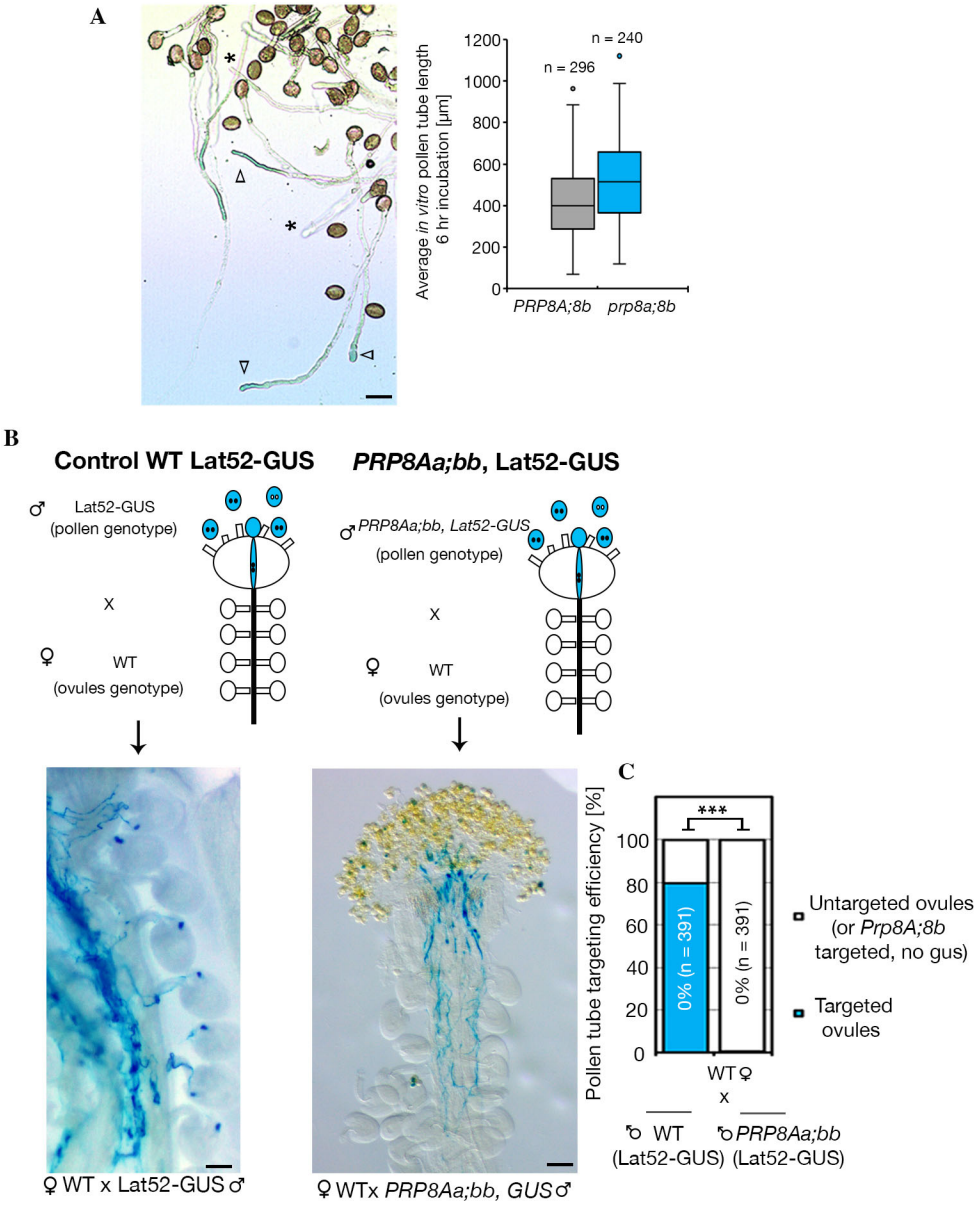


**Fig. 4. PRP8A/PRP8B activity specifies pollen tube competence to target ovules for fertilization.** (A) *In vitro prp8a prp8b* pollen tube growth is not affected. Empty triangles indicate double mutant pollen tubes stained with GUS; asterisks indicate wild-type-like (PRP8A;b) pollen tubes. The box plot shows pollen tube length distribution of the two genotypes. Middle bars are median values, boxes indicate the first to third interquatile ranges, whiskers indicate 1.5 of minimum and maximum interquartiles, and dots indicate outlier values. (B) *In vivo prp8a prp8b* pollen tube guidance towards wild-type ovules is defective. Blue dot assay of the wild-type pistil pollinated with control LAT52pro-GUS expressing pollen (left) or with *prp8a prp8b*-LAT52pro-GUS pollen (right). Note the normal growth of *prp8a prp8b*-Lat52GUS pollen tubes in the entire length of the pistil without ovule targeting or pollen tube burst at the micropyle entry. (C) Blue-dot assay quantification of *prp8a prp8b*-LAT52pro-GUS pollen tube ovule-targeting efficiency. ***$P$<0.001. Scale bars: 50 µm.

gametophyte. Together, our data suggest that PRP8A/PRP8B coordinately regulates pollen tube competence to respond to funiculus and/or micropylar attraction signals secreted by the ovules for pollen tube guidance.

### *prp8a prp8b* double mutant ovules might exhibit abnormal embryo sac

To better understand the defects of *prp8a prp8b* ovules, we emasculated flowers from *PRP8Aa;bb* plants at stage 13-14 with fully developed embryo sacs (Christensen et al., 1997), and left them to mature for 48 h. DIC imaging revealed that mature *prp8a prp8b* double mutant ovules showed a probably malformed embryo sac morphology in ∼35% of the ovules (Fig. 5A-F). Morphologically, the characteristic conical projection associated with the wild-type embryo sac micropyle pole was not observed in *prp8a prp8b* ovules (Fig. 5B). Instead, the *prp8a prp8b* embryo sac appeared to protrude to the very close proximity of the micropyle entry site or be pressed against the inner integuments of the ovule maternal tissues (Fig. 5C,D). In other ovules, the *prp8a prp8b* embryo sac appeared either enlarged or collapsed (Fig. 5E,F). Compared with wild-type dissected ovules at the same stage, only 3% of the ovules showed unusual embryo sac morphology (Fig. 5G). Despite the abnormal embryo sac morphology of *prp8a prp8b* ovules, nuclear staining revealed no obvious defects in nuclear proliferation, nuclear fusion or cellularization (Fig. 5H,I).

To further assess the impact of *prp8a prp8b* on the female gametophyte, we monitored the expression of FGR7.0, an embryo sac triple cell marker for synergid cell-specific (LURE1.2pro-NLS::3×GFP, AT5G43510), egg cell-specific (EC1pro-NLS::3×mCherry) and central cell-specific expression (CRP defensin-like LCR80 DD22pro-NLS::YFP, AT5G38330) (Völz et al., 2013). Live cell imaging in the wild-type embryo sac revealed that 88.5±9% ($n$=357/403) of the ovules showed correct expression of FGR7.0 in all three cell types, with strong expression in the synergid and the egg cell and weak expression in the central cell (Fig. 5J,K). In contrast, only 50.4±3% ($n$=646/1288) of the ovules from *PRP8Aa;bb* dissected pistils correctly expressed the FGR7.0 marker (Fig. 5J,K). Instead, 44.8±4% ($n$=578/1288) of the embryo

Development (2020) 147, dev186742. doi:10.1242/dev.186742

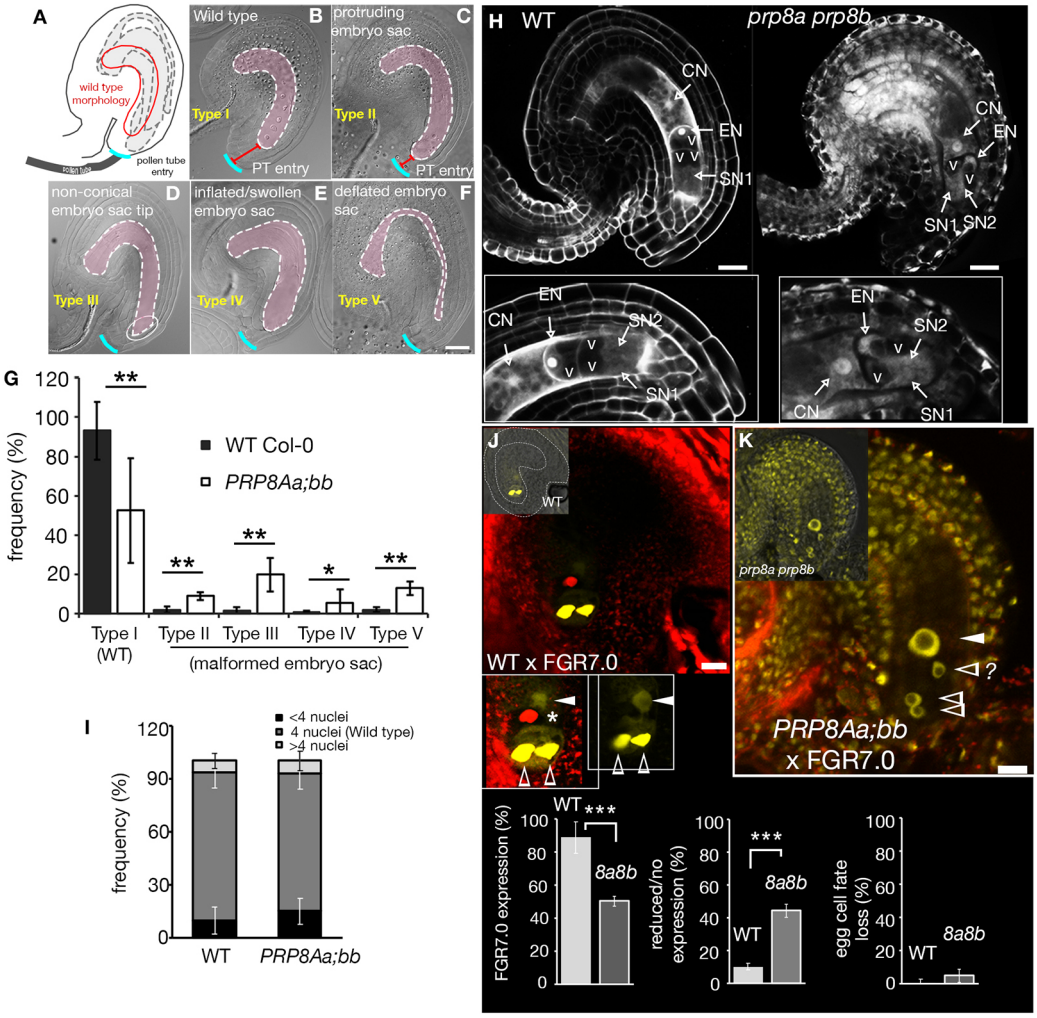


**Fig. 5. Embryo sac morphology and expression of cell-fate markers is impaired in *prp8a prp8b* mutant ovules.** (A) Superimposed cartoon summarizing the morphological defects of the *prp8a prp8b* embryo sac. (B-F) Representative DIC images of ovules dissected from wild-type and *PRP8Aa;bb* pistils at stage 13 of flower development. The embryo sac is highlighted in pink and its vicinity to the micropyle entry (turquoise) is marked by the red T-bone lines. Note the changes in morphology and distance of the embryo sac to micropyle entry. (G) Quantification of classes of defective embryo sac observed. (H) Optical sections from confocal laser scanning microscopy. Autofluorescent nuclei of each cell type of the female gametophyte are shown. Lower panels are at 3× magnification. (I) Frequencies of number of nuclei in wild-type and double mutant *prp8a prp8b* embryo sac at stage 13. (J) Representative expression of triple cell fate reporter markers FGR7.0 in wild-type mature ovules showing strong expression in synergid cells (open triangles), weak expression in the central cell (filled white triangles) and EC1-mCherry expression in the egg cell (asterisk). (K) In contrast, FGR7.0 expression is misregulated in *prp8a prp8b* ovules showing either no expression or stronger expression in the central cell and a loss of egg cell fate in some ovules. Graphs are quantification of FGR7.0 expression in control wild-type and double mutant *PRP8Aa;bb* genotypes. A question mark indicates unknown cell fate of the egg cell, expressing either the synergid or the central cell marker. Data are mean±s.d. ($n$=35). *$P$<0.05, **$P$<0.01, ***$P$<0.001 (Student's $t$-test). CN, central cell nucleus; EN, egg cell nucleus; m, micropyle; SN, synergid cell nucleus; V, vacuole. Scale bars: 50 µm.

sacs from *PRP8Aa;bb* pistils showed no or reduced expression in the synergid and egg cells (Fig. 5J,K). Remarkably, of the *prp8a prp8b* ovules with reduced FGR7.0 expression, 4.9±5% ($n$=64/1288) showed higher FGR7.0 expression in the central cell than in synergid cells, and the egg cell appeared to adopt the expression of either the synergid or the central cell marker and lost EC1-mCherry expression (Fig. 5K). These results imply that PRP8A and PRP8B could redundantly function in regulating gene expression and defining correct cell fate specification during ovule maturation.

### RNA sequencing reveals splicing defects and deregulated gene expression in *prp8a prp8b* ovules

The fact that the *prp8a prp8b* double mutant did not show pleiotropic effects suggests that PRP8A and PRP8B are not strictly constitutive regulators of the splicing machinery. To unveil the extent of affected genes and define the molecular phenotype following *prp8a prp8b* knockdown, we isolated RNA from dissected ovules of *PRP8Aa;bb* pistils and conducted 150 bp paired-end RNA sequencing (RNA-seq) transcript profiling. We analyzed differential gene expression (DGE), intron retention (IR) and differential exon usage (DEU) relative to wild-type ovules. Pearson pairwise correlation clustering confirmed reproducibility of the replicates for individual RNA-seq libraries (Fig. 6A). Using DESeq2 R studio with a false-discovery rate (FDR) of <1%, RNA-seq data revealed that 764 genes (2.9%) were classified as downregulated and 779 genes (3%) were upregulated in *prp8a prp8b* ovules (Fig. 6B). At a Log2 fold change of >2 and $P$<0.05, 321 genes were considered downregulated and 163 genes were classified as upregulated in *prp8a prp8b* ovules (Fig. 6B; Tables S3, S4).

Development (2020) 147, dev186742. doi:10.1242/dev.186742

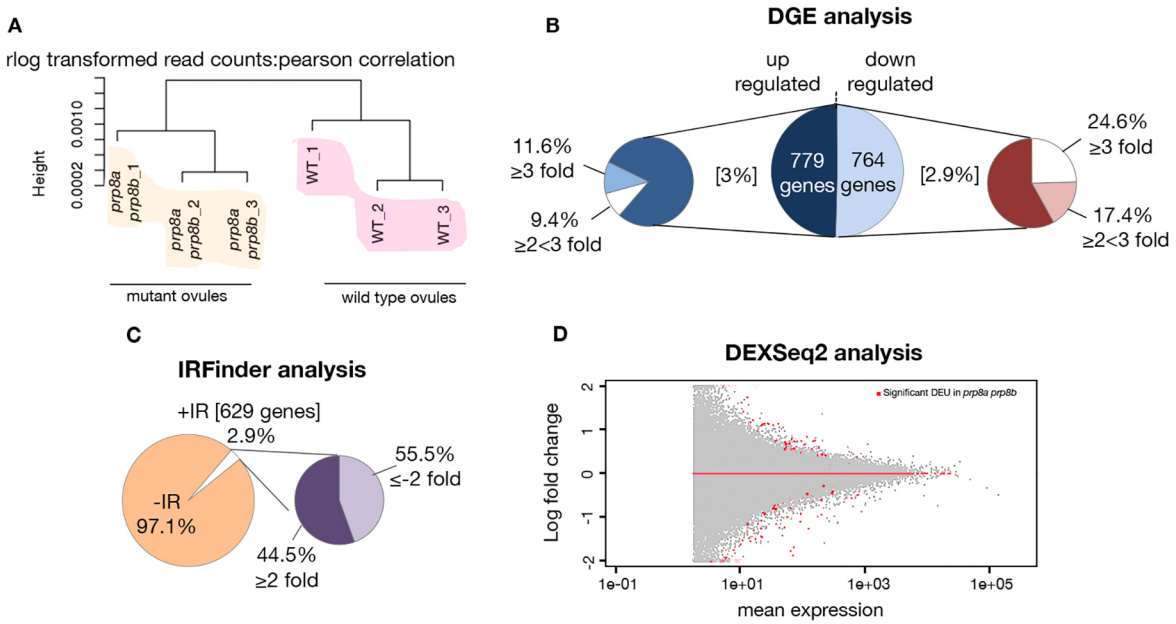


**Fig. 6. *prp8a prp8b* molecular phenotype revealed by RNA-seq.** (A) Clustering of the ovule transcriptome samples based on Pearson pairwise correlation. (B) DGE in *prp8a prp8b* mutant ovules analyzed using DESeq2 and independently complemented with edgeR analysis with $P<0.05$. (C) Frequency of IR in *prp8a prp8b* ovules assessed using IRFinder pipeline at FDR<5%. (D) MA plot of fold change of exon usage versus averaged normalized counts per exon. Red dots are exons with significant DEU at adjusted $P<0.1$.

Analysis of the RNA-seq data with the IRFinder platform identified 629 genes (2.9%) that showed >twofold significant IR in *prp8a prp8b* ovules compared with wild-type ovules (Fig. 6C). Of these, 55% showed reduced IR, whereas 45% showed increased IR events in *prp8a prp8b* ovules (Fig. 6B; Tables S5, S6). Analysis of DEU using DEXSeq R script (Anders et al., 2012) revealed 220 genes that showed significant DEU in *prp8a prp8b* ovules, indicating pre-mRNA mis-splicing in *prp8a prp8b* ovules (Fig. 6D, E; Tables S7-S9). Collectively, the RNA-seq data analyses suggest that PRP8A/PRP8B participates in the pre-mRNA splicing of only the subset of genes that are expressed in ovules.

### PRP8A and PRP8B co-regulate expression of MYB98 and CRP genes

To investigate at the molecular level the likely cause of *prp8a prp8b* defects in pollen tube attraction, we analyzed the RNA-seq data for the expression of genes encoding CRPs, DEFLs, Rapid alkalinization factors (RALFs), MLO proteins and transcription factor MYB98, a family of genes that have been implicated to mediate pollen tube attraction and reception (Dresselhaus et al., 2016; Wang et al., 2017; Higashiyama and Yang, 2017; Leydon et al., 2017). In *prp8a prp8b* ovules, 55 genes belonging to the CRP family were mis-expressed, representing 11% of the total mis-expressed genes in *prp8a prp8b* ovules (Fig. 7A). Of these, 34 genes encode proteins belonging to the low molecular weight CRP subfamily and 21 encode the DEFL protein subfamily (Fig. 7A). Of the 34 mis-expressed low molecular weight CRPs, 8 genes (24%) were upregulated by up to fivefold and the remaining 26 genes (76%) were downregulated by up to sevenfold (Fig. 7A). Of the 21 DEFL subfamily genes, all were downregulated by up to sixfold in *prp8a prp8b* ovules ($P<0.05$, Fig. 7A). Of note, all of the LURE genes, *AtLURE1.1-1.5*, were downregulated in *prp8a prp8b* ovules (Fig. 7A). Similar analysis using edgeR (Robinson et al., 2010) consistently revealed downregulation of *LURE1.1* by 1.3 Log2 fold and *LURE1.2-1.5* by >2 Log2 fold ($P<0.05$) in *prp8a prp8b* ovules.

LURE gene expression is controlled by synergid cell-specific MYB98 transcription factor, which is itself under the regulation of central cell-specific CCG (Chen et al., 2007) and CBP1 (Li et al., 2015). Analysis of our RNA-seq data reliably detected downregulation of MYB98 and upregulation of CBP1 in *PRP8Aa;bb*-derived RNA-seq expression in all three replicates (Fig. 7C). To support this observation, we monitored the expression of MYB98pro-NLS::GFP and MYB98pro-PM::GFP decorating synergid cell nuclei and the plasma membrane, respectively, in *prp8a prp8b* ovules. In contrast to 90.2±5% ($n$=121/134) of positively expressing ovules in wild-type controls, live cell imaging revealed complete downregulation of MYB98pro-NLS:;GFP expression in the synergid cell nuclei of ∽46.9±4% ($n$=444/946) ovules from *PRP8Aa;bb* dissected pistils, representing the *prp8a prp8b* double mutant population (Fig. 7D). We obtained similar results using proMYB98pro-PM:;GFP. Mutants *myb98*, *ccg1* and *cbp1* all result in downregulation of CRPs including LURE gene expression (Okuda et al., 2009; Li et al., 2015). Furthermore, all members of the Egg Cell 1 family were also downregulated in *prp8a prp8b* ovules (Fig. 7C). These results suggest that downregulation of MYB98 is probably the reason why downregulation of LURE and other CRPs impacts pollen tube further circumventing *prp8a prp8b* ovules from any successful gamete fusion and fertilization.

The RALF gene family was recently shown to regulate pollen tube guidance and homeostasis (Mecchia et al., 2017; Ge et al., 2017). In *prp8a prp8b*, *RALF20* was more than fivefold upregulated, whereas *RALF21*, *RALF28* and *RALF29* were up to fivefold downregulated (Fig. 7A). Two *MLO* genes were also identified, *MLO6* was approximately fourfold upregulated and *MLO12* was twofold downregulated (Fig. 7A). However, the promoter activities of *MLO6* and *MLO12* were not active in ovules and were only detected in stigma and style, respectively (Davis et al., 2017).

We then tested whether *AtLURE1.1-1.6*, *FERONIA* (*FER*) and *LORELEI* (*LRE*) genes could be mis-spliced in *prp8a prp8b* ovules.

Development (2020) 147, dev186742. doi:10.1242/dev.186742

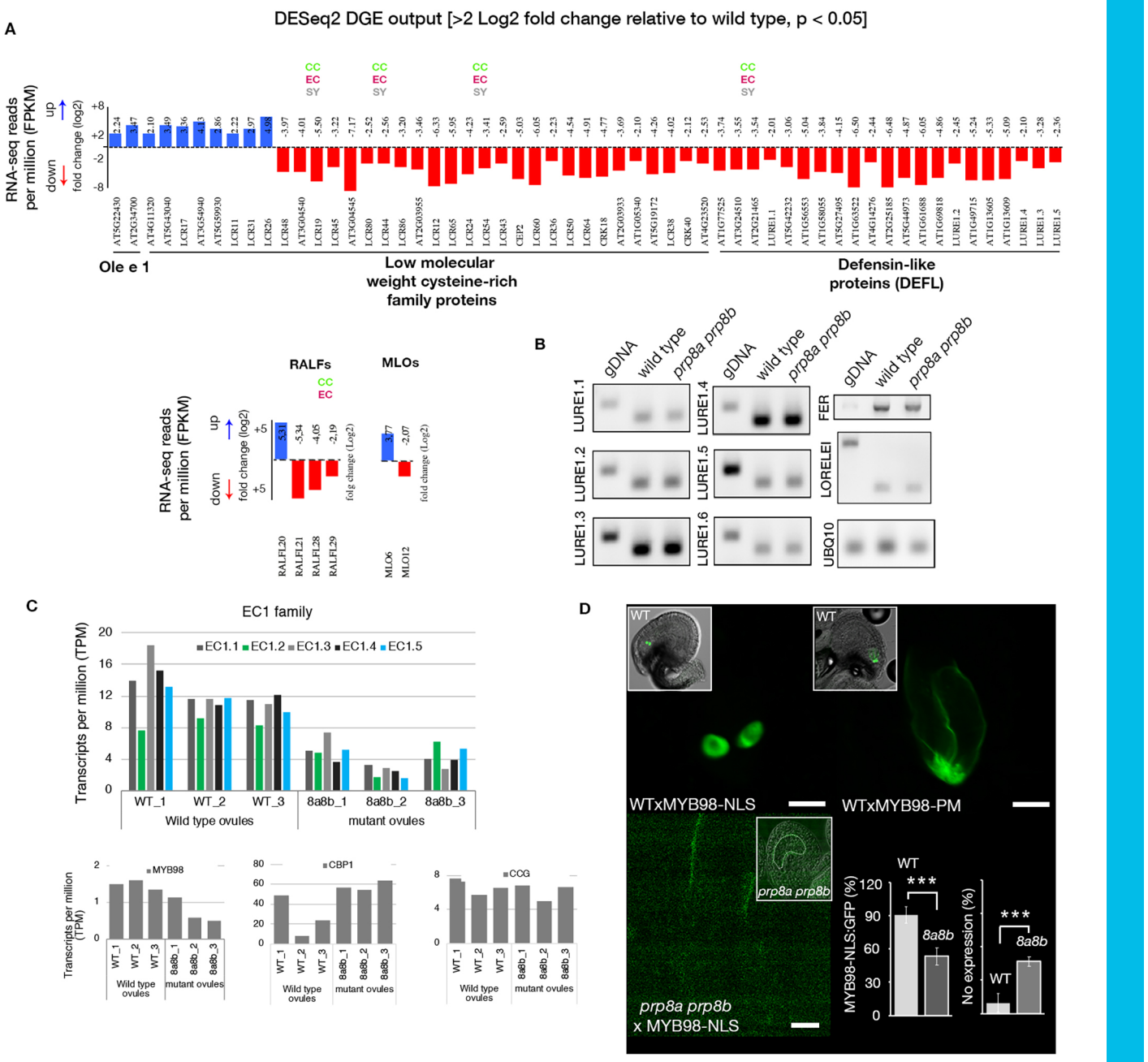


**Fig. 7. MYB98, LUREs and several CRPs are downregulated in *prp8a prp8b* ovules.** (A) DESeq2 differential gene expression RNA-seq analysis reveals several misregulated CRPs at Log2 >twofold, with FDR <5%. Note, however, only four of the CRP genes could be mapped to Wuest et al. (2010) embryo sac cell-specific transcriptome and are all expressed in all three cell types – central cell (CC), egg cell (EC) and synergid cells (SY). (B) Intron profiling by semi-qRT-PCR validated that PRP8A/PRP8B does not regulate splicing of *LURE* genes, *LORELEI* or *FER* in ovules. (C) Normalized ovule RNA-seq data reveals reduced expression of EC1 family members, MYB98 pollen tube attractant and overexpression of CBP1 in *prp8a prp8b* ovules. (D) Validation of *MYB98* mis-expression in *prp8a prp8b* ovules with MYB98pro-NL::GFP and MYB98pro-PM::GFP (plasma membrane). Insets show GFP-bright-field merged image. Graphs show frequency of ovules with GFP expression (left) and those with no detectable expression (right) in respective genotypes. Scale bars: 50 µm.

Intron profiling by semiRT-PCR and a test for the frequency of exon usage (DEU) and IR events revealed no significant alterations in pre-mRNA processing of LUREs, *FER* or *LRE* in *prp8a prp8b* ovules (Fig. 7B; Fig. S3).

It is also evident that protein secretion and the endomembrane system play pivotal roles in pollen tube guidance (von Besser et al., 2006; Li et al., 2011; Hafidh et al., 2016b). We therefore extended our RNA-seq analysis to include genes of the secretory pathways. Analysis of IR frequency revealed a plethora of secretory pathway genes to be aberrantly spliced in *prp8a prp8b* mutant ovules. Among them were genes involved in ER-Golgi transport (*GRIP*), Golgi-vacuole transport for sorting (*DRP2A* and *VSR-1*), Golgi-plasma membrane transport and exocytosis (*SFH3/SEC14* and *EXO70*) (Fig. S4). Additional secretory genes were identified as showing statistically significant DEU compared with wild-type controls, including *SFH3*, *Got1/SFT2*, DUF ER vesicle transporter (AT1G36050) and *AtRABC2b* (Fig. S4). In summary, our RNA-seq data revealed downregulation of upstream regulators of LURE gene expression and a plethora of other CRPs as well as aberrant splicing of key secretory pathway genes in *prp8a prp8b* ovules, which might

Development (2020) 147, dev186742. doi:10.1242/dev.186742

impair secretion of CRPs and therefore exacerbate the pollen tube attraction defects of *prp8a prp8b* ovules.

### PRP8A/PRP8B splicing activity targets more central cell expressed genes

To investigate whether there is a cell-biased effect within the embryo sac following *prp8a prp8b* loss of function, we mapped all of the affected genes from IR, DGE and DEU to the female gametophyte RNA-seq transcriptome from Wuest et al. (2010). Of the 629 genes showing IR in *prp8a prp8b* ovules, 567 (90%) could be mapped to the female gametophyte transcriptome, of which 214 IR genes (34%) were classified as reliably expressed in all three replicates in at least one female gametophyte cell type – synergid cell, central cell or egg cell (Fig. 8A; Supplementary Dataset 2B). We observed that 79 genes (36.9%) with significant IR were central cell-specific, 38 genes (17.8%) were egg cell-specific and no genes with significant IR were identified to be synergid cell-specific (Fig. 8A; Supplementary Dataset 2B). This distribution implies that *prp8a prp8b* splicing defects impact central cell expressed genes twice as much as egg cell encoded genes. In comparison, of the 484 genes that showed significant DGE, 280 genes (58%) could be mapped to the female gametophyte transcriptome (Fig. 8A). Of these, 43 genes (8.9%) were reliably expressed in all three replicates in at least one female gametophyte cell type (Fig. 8A). Unlike IR events, DGE was less biased on cell type-specific deregulated expression (Fig. 8A). Similar results were also obtained with genes

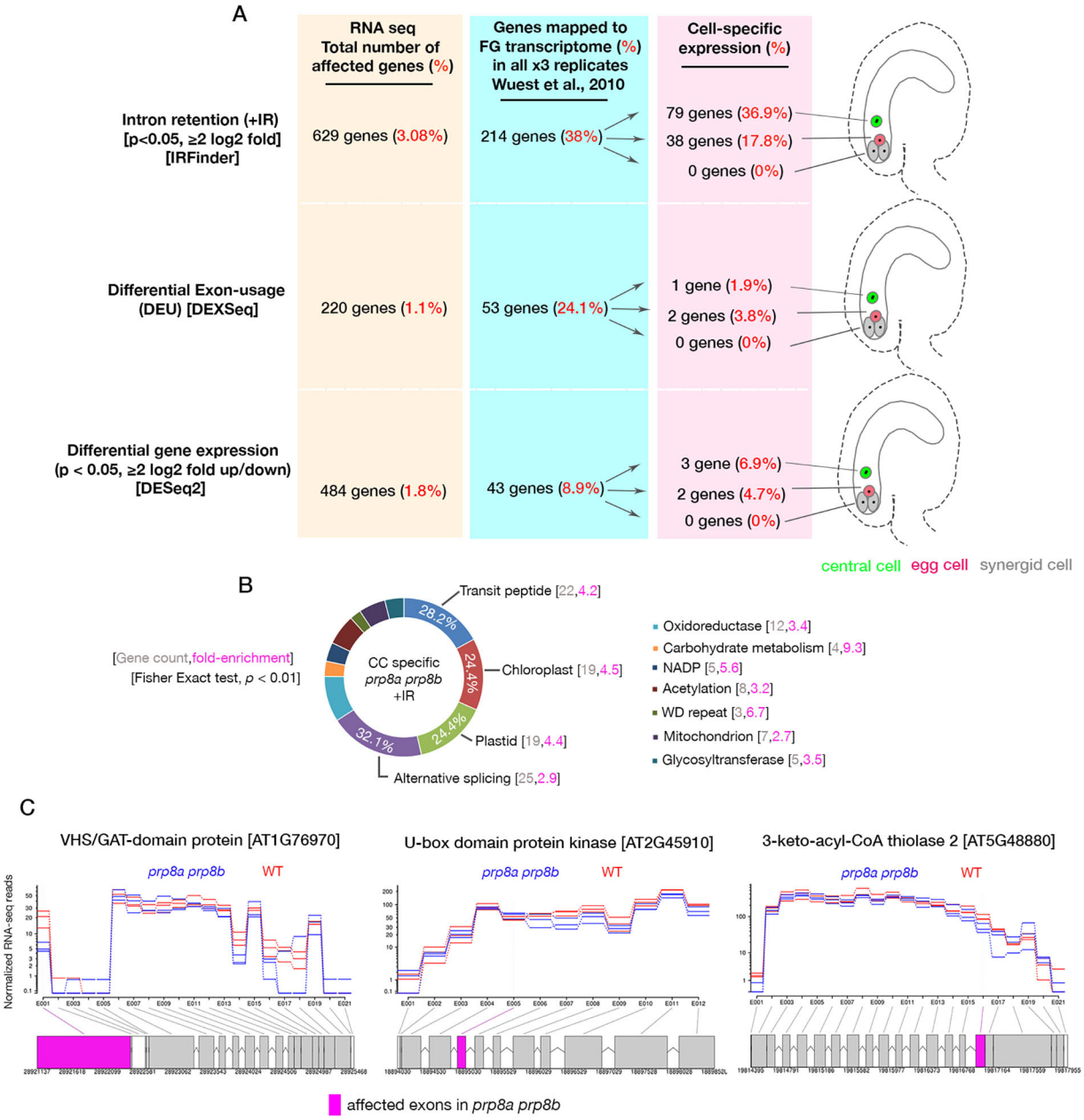


**Fig. 8. *prp8a prp8b* intron retention effect impacts more central cell expressed genes.** (A) Mapping of misregulated genes in *prp8a prp8b* ovules based on their cell type-specific expression according to Wuest et al. (2010) embryo sac cell-specific expression data. (B) Enriched keywords of the IR affected central cell genes, including the number of genes and fold enrichment for each category. (C) DEU of exemplified embryo sac-specific genes, highlighting affected exons in *prp8a prp8b* ovules.

Development (2020) 147, dev186742. doi:10.1242/dev.186742

showing DEU, in which 53 genes (24.1%) of the 220 genes that exhibited significant DEU were reliably expressed in the female gametophyte but showed no significant bias for cell type-specific effects (Fig. 8A). Keyword enrichment analysis ($P$<0.01) of central cell genes with significant IR highlighted genes involved in alternative splicing, transit peptide and chloroplast/plastid differentiation as among the predominantly affected genes (Fig. 8B). Of the genes showing DEU, the gene encoding VHS/GAT-domain protein was identified as central cell-specific, and genes encoding U-box domain protein kinase and 3-keto-acyl-coA thiolase were identified as egg cell-specific (Fig. 8B). These results imply that *prp8a prp8b* loss of function predominantly affects central cell expressed genes through IR as the most common molecular phenotype within the embryo sac.

### Mutant *prp8a prp8b* ovules display differential exon usage of female gametophyte expressed genes and embryo sac developmental genes

To assess the possible molecular phenotype resulting in the *prp8a prp8b* embryo sac morphological defects, we searched the RNA-seq data with emphasis on mRNAs known to regulate embryo sac development (Pagnussat et al., 2005). Using DEXSeq analysis, genes of diverse subcellular roles were identified to show differential exon usage compared with their expression in wild-type ovules. Identified genes included those encoding plasma membrane signaling proteins (GPI-anchored protein), transcription factors and chromatin remodeling factors (DEIH-box helicase and COL13), metabolic enzymes (ATPHS2), splicing factors (PWI-domain splicing factor) and signaling kinases (CPK29) (Figs S5A and S6). More specifically, we identified 12 genes with a direct role in female gametophyte and embryo sac development to be differentially spliced, showing DEU, IR or changes in gene expression (Fig. S6). DEU-informed RNA-seq highlighted *EMBRYO SAC DEVELOPMENT ARREST 9* (*EDA9*, also known as *PGDH1*, AT4G34200), *EMBRYO SAC DEVELOPMENT ARREST 30* (*EDA30*, AT3G03810) and *MAP3K EPSILON PROTEIN KINASE 1* (*MAP3Kε1*, also known as *M3KE1*) to show statistically significant DEU in *prp8a prp8b* ovules (Fig. S5). EDA9 is a 3-phosphoglycerate dehydrogenase that is essential for embryo and pollen development, and *eda9* mutant ovules are arrested at the two-nuclei stage of embryo sac development (Pagnussat et al., 2005). EDA30 is a O-fucosyltransferase family protein that is essential for polar nuclei fusion (Pagnussat et al., 2005). MAP3Kε1 is expressed in developing ovules and the double mutant *map3kε1 map3kε2* displays plasma membrane irregularities in pollen grains, which result in pollen lethality (Chaiwongsar et al., 2012; Mithoe et al., 2016). Post fertilization, MAP3Kε1 is a downstream regulator of the YODA MAP kinase signaling pathway and is essential for the specification of suspensor cell fate at the 1-2 cell stage of zygote development (Bayer et al., 2009). IR and DGE analyses identified additional embryo sac developmental genes that showed either significant intron retention (±IR ≥twofold, $P$<0.05) or downregulation of their transcription in *prp8a prp8b* mutant ovules (≥twofold change, $P$<0.05) (Fig. S6).

### PRP8A and PRP8B exhibit autonomous regulation of their pre-mRNA splicing and splicing of other spliceosome factors

Because PRP8A and PRP8B are subunits of the spliceosome machinery, we investigated whether the spliceosome complex is autonomously regulated by analyzing the RNA-seq data to compare the splicing patterns of *PRP8A* and *PRP8B* in *prp8a prp8b* ovules. DEU analysis revealed that exons 1-3 and 18-20 of *AtPRP8A* were differentially expressed in *prp8a prp8b* mutant ovules, suggesting defective splicing of PRP8A pre-mRNA (Fig. S5B), whereas *AtPRP8B* showed significant differential expression of exon 19 (Fig. S5B). DEXSeq also revealed differential expression of exon 10 of a PIWI domain-containing splicing factor (AT2G29210) (Fig. S5A). IRFinder further revealed mis-splicing of two genes encoding SER/ARG-rich protein splicing factor 34 (SRP34) and SRP34A in *prp8a prp8b* ovules, among other spliceosome subunits encoding genes (Fig. S5C). SRP34 regulates alternative splicing through binding in exonic enhancer and suppressor elements. Our results identified autoregulation of core subunits of the spliceosome machinery that probably culminate in the molecular phenotype of *prp8a prp8b* knockdown.

### PRP8A co-immunoprecipitates with U2-associated SF3A1 splicing enhancer

In humans and yeast, the N terminus of PRP8 interacts with the core of the NineTeen Complex (Prp19/NTC) for activation of the spliceosome machinery, whereas the two domains at the C-terminal tail, the JAB1 (MPN) domain and the U6-RNaseH domain, interact with BRR2 U5-snRNP, U2-snRNPs such as the human homolog of SF3A1 (Tresini et al., 2015; Zhang et al., 2017), and human SLU7 step II factor for selection of the 3′-splice site junction (Zhang et al., 2017). Because the T-DNA insertions in both *prp8a*-12 and *prp8b*-1 interrupt the U6-RNaseH domain, resulting in female and male sterility, we tested whether the relationship between PRP8 and U2-snRNPs identified in human is also conserved in plants to get a hint on PRP8A/PRP8B mechanisms of action. We co-expressed pro*PRP8A-PRP8A*::GFP with *AtSF3A*1-mCherry (AT1G14650) in *Arabidopsis* roots. PRP8A-GFP colocalized with AtSF3A1-mCherry in a gradient-dependent manner within the nuclei of all cells at the root tip (Fig. 9A). Close observation of nuclear speckles confirmed that PRP8A and AtSF3A1 colocalized in some subdomains of the nuclei, but they also formed distinct subdomains within the nucleoplasm (Fig. 9A). Using these stable lines, we then performed *in vivo* co-immunoprecipitation (Co-IP) experiments using a nuclear-enriched proteome subfraction and a total cytosolic proteome from 7-day-old seedlings expressing pro*PRP8A-PRP8A::GFP* as a bait. Western dot blot analysis of PRP8A immunoprecipitated proteins revealed that the PRP8A-GFP complex strongly co-immunoprecipitated with AtSF3A1 in the nuclear-enriched and total fractions, suggesting that PRP8A associates with SF3A1 in *Arabidopsis* (Fig. 9B). We further observed similar affinity Co-IP of PRP8A with histone H3 variant (Fig. 9B). In humans, histone modifications, in particular H3K36me3 and H3K4me3, are strongly linked with alternative splicing through interaction of Histone adaptor (MRG15) and PTB-dependent exon inclusion (Luco et al., 2010, 2011), and recent reports have demonstrated association of several histone variants with splicing factors (Xu et al., 2018). A nuclear localized Translationally Controlled Tumor protein 1 (TCTP1), a non-spliceosome subunit from *Arabidopsis*, was used as a negative control to ensure Co-IP specificity (Fig. 9B). Our results revealed that AtPRP8A associates with U2-snRNP SF3A1 and histone H3 in *Arabidopsis*. We next investigated whether AtPRP8A associates with AtSF3A1 via direct interaction. We performed ratiometric biomolecular fluorescence complementation (rBiFC) (Grefen and Blatt, 2012) with AtPRP8A-nYFP and AtSF3A1-cYFP in *N. benthamiana* leaves. As a positive control, we included TCTP1-nYFP and CPN60-cYFP interaction. We observed no reconstitution of the YFP fluorophore when PRP8A-nYFP and SF3A1-cYFP were co-expressed (Fig. 9C). The lack of interaction indicates that in *Arabidopsis* PRP8A might be weakly or indirectly associated with SF3A1

Development (2020) 147, dev186742. doi:10.1242/dev.186742

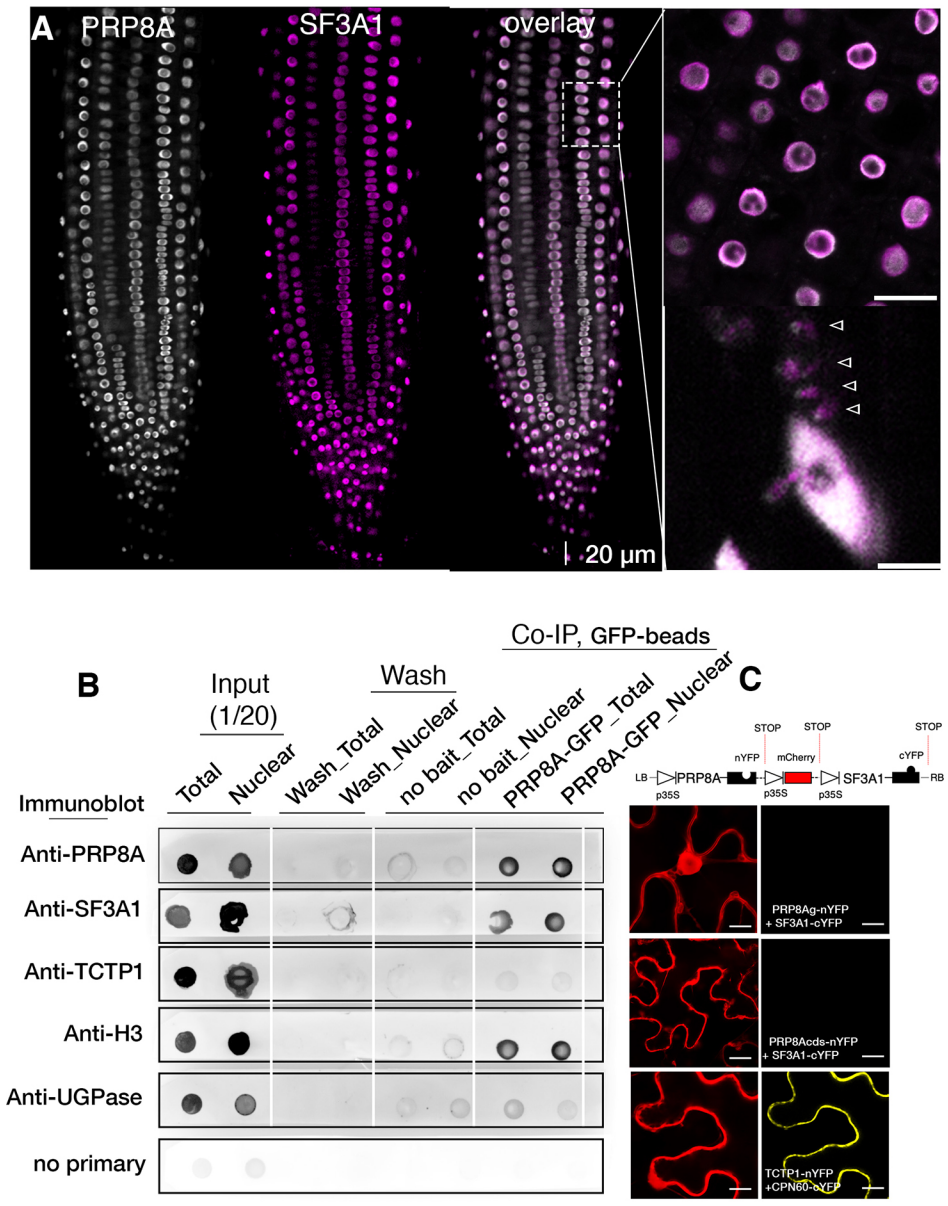


**Fig. 9. PRP8A colocalizes and immunoprecipitates with SF3A1.** (A) Colocalization of PRP8A-GFP with SF3A1-mCherry in 4-day-old *Arabidopsis* roots. Within the nuclear domain, PRP8A also localizes in unique subnuclear foci that do not colocalize with SF3A1 (indicated by triangles). Inset shows higher magnification of boxed area. (B) Western dot blot analysis of PRP8A-SF3A1 by *in vivo* Co-IP. SF3A1 was pulled down by PRP8A-GFP and detected by immunoblotting with anti-PRP8A, anti-SF3A1 and anti-Histone H3 antibodies. TCTP1 (AT3G16640) was used as a negative control. Histone H3 and UGPase antibodies served as nuclear and cytoplasmic markers, respectively. (C) Ratiometric BiFC assays reveals that PRP8A does not physically interact with SF3A1 in *N. benthamiana* leaves. PRP8A-nYFP, either as a full length genomic or full length cDNA, was co-expressed with SF3A1-cYFP in leaves of *N. benthamiana*. TCTP1-CPN60 interaction was used as a positive control for rBiFC. mCherry was used as a marker for monitoring successful expression. Scale bars: 40 µm (A); 5 µm (C).

## DISCUSSION

The spliceosome complex required for pre-mRNA splicing functions uniquely in a tissue- and developmental-specific manner and some of its subunits have been genetically characterized as essential regulators of gamete development (Gross-Hardt et al., 2007; Moll et al., 2008; Staiger and Brown, 2013). In mice, alternative splicing of acrosomal matrix protein, preacrosin-binding protein (ACRBP), plays an essential role in the formation of secretory functional acrosome and competent sperm cells capable of fertilization (Kanemori et al., 2016). In *Drosophila*, a mutation in the NTC/Prp19 pre-spliceosome complex specifically impairs pre-mRNA splicing of early zygotic but not maternally encoded transcripts, suggesting spatiotemporal regulation of the spliceosome subcomplexes (Guilgur et al., 2014). In *Arabidopsis*, *lachesis* mutants (*lis*) with depleted U4/U6 splicing factor PRP4 are defective in lateral inhibition of accessory cell development, resulting in accessory cells with gametic cell fate identity (Gross-Hardt et al., 2007), whereas CLOTHO/GAMETOPHYTIC FACTOR 1 (CLO/GFA1), a U5 subunit of the spliceosome machinery and interactor of PRP8A (Liu et al., 2009), is specifically required for egg and central cell fate specification and tissue-specific expression of LIS (Moll et al., 2008). Similarly, *ATROPOS* (*ATO*, *SF3A60*) encodes a human homolog of SF3a60, a subunit of the SF3Aa-U2 complex. SF3Aa1 is a member of the SF3a-U2 complex and co-immunoprecipitates with PRP8A (Fig. 9). The *ato* (*sf3a60*) mutant is female gametophytic lethal and also shows severe reduction in male transmission with a maximum of 17.44% transmission efficiency (Moll et al., 2008). At ovule maturity, 20% of *ato* (*sf3a60)* embryo sac contained less than seven nuclei and the two female gametic-cell fate markers were deregulated (Moll et al., 2008). In this study, the *prp8a prp8b* double mutant embryo sac might have lost synergid and egg cell fates by not expressing MYB98, LURE1.2 and EC1 markers (Figs 5 and 7). Unlike *lis/gfa1* or *ato*, the *prp8a prp8b* double mutant does not show early gametophytic developmental defects. Even though GFA1 interacts with PRP8A (Liu et al., 2009) and both are components of the U4/U6.U5 tri-snRNP (Bartels et al., 2002; Staiger and Brown, 2013), the lack of direct phenocopy between

Development (2020) 147, dev186742. doi:10.1242/dev.186742

*prp8a prp8b* double mutant and the *gfa1*, *lis* or *ato* (*sf3a60*) mutants, exemplifies the complex regulation of the spliceosome individual subunits and non-universal role of the spliceosome machinery. The phenotype with closest resemblance to the *prp8a prp8b* double mutant phenotype is that of the *ato* (*sf3a60*) mutant, which might explain the close association of PRP8A with SF3aA1 (Fig. 9).

Moreover, PRP8A and PRP8B are fully redundant in their function in the gametophyte, as shown by the normal transmission of *prp8a* and *prp8b* single mutations and the finding that proPRP8A-PRP8A::3UTR and proPRP8B-PRP8B::GFP could fully complement *prp8a prp8b* fertilization defects (Fig. 2). However, this redundancy is restricted to the gametophyte, as *prp8a* alone is embryo lethal (Schwartz et al., 1994; Meinke et al., 2008). Our results suggest that PRP8A/PRP8B spliceosome subunits are selectively involved in splicing of subsets of pre-mRNAs with cell and developmental specific roles, and unlike other U4/U6.U5 tri-snRNP splicing subunits, PRP8A/PRP8B function might not be essential for early gametophyte development.

### Intron mis-splicing predominates in central cell-expressed genes in *prp8a prp8b*

The post-transcriptional effect in *prp8a prp8b* ovules revealed a combined effect on intron splicing and DEU of approximately 4.18% (849 genes) compared with 1.8% (484 genes) on DGE at ≥twofold (Fig. 8). This observation suggests that PRP8A/PRP8B directly participates in intron splicing of ovule-expressed genes and that *prp8a prp8b* knockdown probably has an indirect effect on altered gene expression. In support, we have shown that PRP8A co-immunoprecipitates with a human homolog of SF3A1 as well as with histone H3 variant (Fig. 9). How histones influence splicing was not known until recently. In humans, histone modifications such as H3K4me3, H3K9me3, H3K36me3 and H3acetyl all positively influence recruitment of histone adaptor proteins MRG15, GCN5, CHD1 and HP1$\alpha$ that facilitate recruitment of splicing factors Polyuridine (polypyrimidine tract binding protein) binding proteins (PTB), U2 snRNP and hnRNPs to influence exon inclusion and alternative splicing (Luco et al., 2011). This was exemplified through splicing of two PTB-dependent mutually exclusive exons of human fibroblast growth factor receptor 2 (FGFR2) where two histone modifications, H3K36me3 and H3K4me1, act antagonistically to influence exon inclusion or exclusion, respectively. Moreover, crosslinking and immunoprecipitation experiments have demonstrated direct interaction of histone variants H1, H2A, H2B, H3 and H4 with splicing factors Rbfox2, Rbfox3 and proline- and glutamine-rich protein (SFPQ) (Kim et al., 2018). In plants, the direct link between alternative splicing and either chromatin structure or RNA Pol II elongation rates has yet to be demonstrated; however, recent studies in *Arabidopsis* have shown a positive correlation (Cui et al., 2017).

The observed biased effect on intron splicing over gene expression in the *prp8a prp8b* embryo sac extended to a cell type-specific origin in the female gametophyte. Assessment of the IR events of only genes expressed in all three replicates of the female gametophyte (214 genes of the 397 IR genes; Fig. 8) revealed that genes confined in the central cell are twice as affected on their intron splicing (79/214 genes, 36.9%) compared with those encoded by the egg cell (17.8%) (Fig. 8; Supplementary Dataset 2B). No affected genes were specific to the synergid cell; however, several genes expressed in the synergid cells were also mis-spliced (Fig. 8; Supplementary Dataset 2B). The central cell has a direct role in pollen tube attraction. Mutations in central cell-specific genes *ccg* (Chen et al., 2007), *cbp1* (Li et al., 2015), *maa3* (Shimizu et al., 2008) or *gex3* (Alandete-Saez et al., 2008) completely abolished pollen tube attraction. CCG (Chen et al., 2007) and CBP1 (Li et al., 2015) are thought to mediate pollen tube attraction by regulating transcription of synergid cell-specific MYB98 transcription factor, an upstream regulator of *LURE1* transcription (Okuda et al., 2009; Li et al., 2015). We propose that aberrant splicing of central cell-encoded genes, together with those affected in the synergid cells, might kick-start the molecular cascade leading to loss of *prp8a prp8b* ovule competence in pollen tube attraction. Although mis-splicing is the major event observed in *prp8a prp8b*, particularly in the central cell, it is difficult to draw a conclusion about whether this is the major factor (over changes in gene expression) leading to pollen tube attraction defects and lack in fertilization of *prp8a prp8b* ovules.

### Downregulation of MYB98 and CRPs could be the hallmark cause of pollen tube attraction defects in *prp8a prp8b*

Although there was a prevalent effect on pre-mRNA splicing in *prp8a prp8b* double mutant ovules, transcripts encoding CRPs stood out the most, representing 20% (55/284 genes) of the total downregulated genes by ≥twofold (Fig. 7). Upstream of CRPs, our RNA-seq data supported by the MYB98pro-NLS::GFP reporter constructs revealed downregulation of MYB98 and upregulation of CBP1, both of which are essential transcriptional regulators of LURE CRPs and pollen tube attraction (Fig. 7) (Kasahara et al., 2005; Okuda et al., 2009; Li et al., 2015). CRPs are the major family of proteins that have been implicated to function directly in pollen tube attraction (Higashiyama and Yang, 2017). Among the downregulated CRPs, are all six members of the LURE subfamily expressed in the synergid cell (Fig. 7). Also, of significant note, three out of four of the central cell-specific CRPs that are also downregulated in *ccg* and *cbp1* pollen tube attraction mutants, DOWN-REGULATED IN *dif*22 (*DD22*, *LCR80*, At5g38330), *DD36* (At3g24510) and AT3G04540, were also downregulated by >2.5-fold in *prp8a prp8b* ovules (Fig. 7). In line with the misregulation of CRPs in *pr8a prp8b* ovules, we detected ectopic promoter activities of a pollen-specific CRP Ole e 1 subfamily gene LAT52, LAT52pro-GUS, initially in *prp8a prp8b* ovules and later confirmed in *prp8a* single mutant ovules (Fig. S2). LAT52 is secreted by pollen tubes and functions as a ligand perceived by pollen-specific receptor-like kinases (RLKs), PRK2 and PRK4, to regulate pollen tube growth by endocrine signaling (Tang et al., 2002; Muschietti et al., 1994; Hafidh et al., 2016a,b). The −572 bp LAT52 promoter fragment confers transcriptional regulatory elements that provide pollen (vegetative cell) specificity and enhanced transcriptional activity specifically in pollen (Twell et al., 1990, 1991). The ectopic activation of LAT52 expression in ovules culminates in the effect of the *prp8a prp8b* molecular phenotype on CRPs misregulation. It will be informative to further investigate which other male-specific expressed genes are ectopically activated in *prp8a prp8b* ovules. This will be key in defining the sexual identity and cell-fate specification of *prp8a prp8b* ovules. We propose that the downregulation of MYB98 and many CRPs is most likely the hallmark cause of the pollen tube attraction defects observed in *prp8a prp8b* ovules.

### Conclusions

This work has uncovered a molecular signature through which PRP8A/PRP8B subunits act redundantly to define male-female signaling competence for successful pollen tube attraction in *Arabidopsis*. PRP8A/PRP8B facilitates pollen tube attraction by

Development (2020) 147, dev186742. doi:10.1242/dev.186742

controlling transcription of LURE pollen tube attractants and several other CRP genes via MYB98 transcriptional regulation as well as through splicing of predominantly central cell-expressed genes (Fig. S7). These defects in *prp8a prp8b* double mutants might be coupled with loss in female gametic cell fate specification at ovule maturity and thus could contribute to overall ovule incompetence for pollen tube attraction. It will be important to uncouple these two events and establish how PRP8A/PRP8B controls pollen tube pathfinding competence to achieve successful fertilization. Collectively, the results hint at a spliceosome autoregulation mechanism and provide a potential pathway to isolate upstream regulators for pollen tube attraction.

## MATERIALS AND METHODS

### Plant material and growth conditions

*Arabidopsis thaliana* plants were grown at 22°C and 60% humidity in Conviron PGC Flex growth chambers under 16 h light/8 h dark conditions. Seeds of Col-0 wild-type (WT), PRP8A (At1g80070) and PRP8B (At4g38780) plants were obtained from The European Arabidopsis Stock Centre. T-DNA insertion lines SAIL_274_D02 T-DNA (*prp8a*-12), SALK_085295C and SALK_085295 (*prp8b*-3), SALK_044221C and SALK_044221 (*prp8b*-1) and SAIL_100_G10 (*prp8b*-2) were used in this study. T-DNA insertion lines were genotyped using SALK LBb1.3 and SAIL LB2 oligonucleotides in combination with gene-specific oligonucleotides (Table S1). The exact positions of the T-DNA insertions were established by sequencing and are marked in Fig. 2A.

### RNA-seq library construction and sequencing

Ovules were isolated by dissecting flowers from stage 13-14 (FG7) containing a fully developed embryo sac (Christensen et al., 1997) from *PRP8Aa;bb* double mutant plants and wild-type control plants. RNA extracted from three biological replicates of each was used for Next Generation (NGS) RNA Sequencing. Total RNA was isolated from dissected ovules using Qiagen Plant RNA extraction kit (Qiagen). Total RNA was treated with DNase (Ambion) and RNA integrity (RIN) analyzed using a bioanalyzer. RNA (800 ng) with RIN >7 was processed using TrueSeq stranded total RNA library with RiboZero plant prep kit (Illumina, San Diego, CA, USA) as per the manufacturer's protocol. Samples were run on HiSeq4000 2×100 bp paired-end run Illumina sequencing machine (Illumina, San Diego, CA, USA) by Macrogen (Geumcheon-gu, Seoul, South Korea).

### mRNA-seq data analysis

The raw sequenced data were subjected to quality control and trimming using FastQC and Timmomatic (Bolger et al., 2014). Resulting reads were mapped to the TAIR 10 genome with STAR aligner, version 2.6 (Dobin et al., 2013) using default parameters. The Feature Count program from the subread package, version 1.6.2 (Liao et al., 2014) was used to generate the count matrix by following steps described in the documentation.

R programs DESeq2, version 1.22.1 (Love et al., 2014) was utilized to determine DGE and DEXSeq, version 1.28.0 (Anders et al., 2012) was used to determine DEU between wild-type and *prp8a prp8b* mutant plants. The count matrix was used as inputs in DESeq2. False discovery rates (FDR) were calculated for gene-specific *P*-values of <0.05 using the Benjamini–Hochberg method (Benjamini and Hochberg, 1990). Gene expression levels were then quantified using rlog normalized counts.

Counts, as input for DEXSeq, were prepared with included Python scripts. The generalized linear model (GLM) was used to detect DEU with FDR adjusted to the overall gene expression level with $P<0.1$. IRFinder (Middleton et al., 2017) with default parameters was applied to determine differentially retained introns between the wild-type and *prp8a prp8b* double mutant. Introns were considered differentially retained if the Benjamini–Hochberg adjusted *P*-value was <0.05 while the IR ratio was ≥2. All biostatistic analyses were implemented and performed using in-house scripts written in Unix shell and R. For graphical display, all genes identified to show statistically significant exon usage in *prp8a prp8b* ovules are presented in HTML interactive format (Table S7). The data discussed in this article have been deposited in GEO under accession number GSE151462.

### *In vivo* co-immunoprecipitation with nuclei fraction

The full length coding sequences (CDSs) of PRP8A together with its native promoter (997 bp) were amplified and cloned into pB7FWG,0 to create proPRP8A-PRP8A::eGFP constructs. A 35S-AtSF3A1::mCherry construct was a donation from the Andreas Nebenfuhr laboratory (University of Tennessee). For detailed cloning information, see the next section. Stable *Arabidopsis* transformants were generated expressing both constructs. Total proteins from approximately 2 g of 4-day-old seedlings expressing proPRP8A-PRP8A::eGFP and 35Spro-AtSF3A1::mCherry constructs were isolated according to Deng et al. (2016) using Honda lysis buffer (25 mM Tris·HCl pH 7.4, 2.5% Ficoll 400, 5% dextran T40, 0.4 M sucrose, 10 mM $MgCl_2$, 5 mM DTT, and 1× complete protease inhibitor cocktail). The homogenate was filtered through 50 µm nylon mesh to clear larger fragments and Triton X-100 was added to a final concentration of 0.5%. For nuclei enrichment, the flow through was centrifuged at 1500×***g*** for 5 min at 4°C. The pellet was gently resuspended twice with nuclei resuspension buffer (10 mM Tris HCl pH 8.0, 0.25 M sucrose, 10 mM $MgCl_2$, 5 mM β-mercaptoethanol, 1% Triton X-100, 0.1 mM PMSF, protease inhibitors) and centrifuged at 1500×***g*** for 5 min at 4°C. Nuclei were then resuspended in ice-cold nuclei lysis buffer [200 mM $(NH_4)_2SO_4$, 20% glycogen, 25 mM HEPES pH 7.9, 5 mM DTT, 1 mM PMSF, protease inhibitors] and gently mixed for 2 h at 4°C to release the nuclear proteins. The nuclear fraction was centrifuged at 17,950×***g*** for 10 min to remove remaining debris. Total and nuclear-enriched proteomes were used immediately for Co-IP. GFP-Trap-A agarose (Chromotek) was used in subsequent Co-IP assays. The immunoprecipitates were detected by anti-PRP8A (1:1000; Abcam 79237), anti-SF3A1 (1:1000; Abcam 128898), anti-TCTP (1:500; Abcam 37506), anti-H3 (1:1000; Abcam 1791) and anti-UGPase (1:1500; Agrisera AS05086) antibodies. To monitor primary antibodies specificity, strips with omitted primary antibodies were used as negative controls. Appropriate alkaline phosphatase-conjugated anti-rabbit and anti-mouse secondary antibodies were used for detection using nitro-blue tetrazolium chloride (NBT) and 5-bromo-4-chloro-3′-indolyphosphate p-toluidine salt (BCIP) chemiluminescence detection.

### Bimolecular fluorescence complementation analysis

To create ratiometric PRP8Agenomic-nYFP and AtSF3A1-cYFP constructs, a genomic fragment of PRP8A coding sequence and CDSs of SF3A1 from the cDNA of rosette leaves were cloned into the 35Spro:pBiFCt-2in1-CC vector to generate the PRP8Agenomic-nYFP SF3A1cds-cYFP co-expression construct (Grefen and Blatt., 2012). Similarly, CDSs of PRP8A were amplified from leaf cDNA and, together with SF3A1, were cloned into 35S:pBiFCt-2in1-CC vector to generate the PRP8Acds-nYFP SF3A1cds-cYFP co-expression construct. All cloning was performed using multisite gateway technology (Invitrogen). The specific oligonucleotides used are described in Table S1. These constructs were subsequently introduced into *Agrobacterium* strain GV3101 and used for infiltration into leaves of *N. benthamiana*. After transformation, plants were grown in light condition for 48 h before observation. The YFP fluorescence was observed using a Zeiss LSM880 microscope.

### Constructs and plant transformation

All PCRs to amplify cloned fragments were performed using high-fidelity Phusion polymerase (New England Biolabs) according to the manufacturer's instructions. Oligonucleotide sequences are listed in Table S2. For the full-length PRP8A-GFP under native promoter, a fragment of 14,523 bp, including 997 bp of promoter and 5′UTR, was amplified with/without stop codon, cloned into the pENTR/D-TOPO vector and recombined into the destination vector pK7FWG,0 (Karimi et al., 2002) bearing the eGFP marker to generate the proPRP8A-PRP8A::eGFP construct. To generate proPRP8A-PRP8A-3′UTR, extended 3′-end oligonucleotides were used to incorporate the 498 bp 3′UTR and the entry clone was used in LR reaction with pH7FWG,0 backbone to generate the proPRP8A-PRP8A-3′UTR expression construct. Full-length proPRP8B-PRP8B::GFP was amplified and cloned using a similar approach. All constructs were transformed into *Arabidopsis* via floral dipping (Clough and Bent, 1998).

Development (2020) 147, dev186742. doi:10.1242/dev.186742

### Transmission analysis

*PRP8Aa* heterozygous plants were back-crossed into Col-0 wild-type background for determining female transmission and crossed into male sterile *ms1*-/- (Yang et al., 2007) to study male transmission. To generate the *PRP8Aa;bb* double mutant plants, flowers of *PRP8Aa* were emasculated and pollinated with homozygous *prp8bb* pollen grains; inversely, *prp8bb* flowers were emasculated and pollinated with *PRP8Aa* pollen grains. For transmission analysis of the double mutant, *PRP8Aa;bb* flowers were emasculated and pollinated with Col-0 wild-type pollen grains and used to calculate female transmission efficiency. In addition, pollen grains from the *PRP8Aa;bb* double mutant plants were used to pollinate male sterile *ms1*-/- pistils and the resulting progeny used to calculate male transmission efficiency. Progeny of these crosses were genotyped by PCR for the presence of T-DNA insertion and the transmission efficiency calculated.

### Imaging of embryo sacs

Stage 12a (FG1) and stage 13-14 (FG7) flowers (Christensten et al., 1997) were dissected on double-sided tape. The placentas bearing the developing ovule primordia were excised and placed immediately in chloral hydrate clearing solution. After 2 days, the fixative was removed and the placental strands mounted onto microscope slides in a 30% glycerol solution. During mounting, the two placental strands were separated and excess tissue was removed. Ovule primordia were observed under Zeiss AxioImager Apotome 2. Images were collected with a 40×/1.2 W C-Apochromat objective.

### Live cell imaging of *prp8ab* ovules

Pistils from *PRP8Aa;bb* were emasculated and left to mature for 2 days. Emasculated pistils as well as control *ms1* pistils were pollinated with pollen expressing the LAT52pro::GFP;HTR10pro::RFP marker line. After 24 h, pollinated pistils were placed on double sided tape and the placentas bearing developing ovule primordia were excised with a 25 G needle and placed immediately on a microscope slide on a drop of 30% glycerol. Fertilization events were captured using a Zeiss LSM 880 confocal laser scanning microscope with C-Apochromat 40×/1.2 WI, excitation 514 nm, emission recorded 566-719 nm for the red channel and excitation 490 nm and emission recorded 509-520 nm for the green channel. Representative single slice confocal sections were used for presentation. Image processing was done using a Fiji application.

### Analysis of ovule attractivity by aniline blue staining

Pistils were harvested at 18 HAP and subjected to aniline blue staining as described below. Samples were analyzed by Zeiss Axioimager Apotome2 and images captured with ZEN software.

### Pollen viability stain and aniline blue staining

For aniline blue staining, pistils of self-pollinated wild-type and *PRP8Aa;bb* plants or cross-pollinated *ms1* plants with wild-type or *PRP8Aa;bb* pollen were stained for callose according to the protocol of Mori et al. (2006).

### Confocal and DIC microscopy

For mutant embryo phenotypic screening, seeds were cleared in a solution of chloral hydrate. Overnight clearing was sufficient for all developmental stages. Samples were observed under the DIC optics on a Nikon TE-2000 microscope. Images were processed in the NIS Elements software (LIM). Confocal images were taken on a Nikon Eclipse Ti confocal microscope equipped with CSU-X1 spinning disk module and Andor iXon3 EMCCD camera, as well as with a Zeiss LSM880 confocal microscope, and captured with ZEN 2.3v software. Images were analyzed and assembled with ImageJ/Fiji (http://imagej.net/http://fiji.sc/Fiji), Adobe Photoshop CS6 (www.adobe.com), Ink-scape (www.inkscape.org) and NIS Elements (LIM) software.

### Blue dot assay

Young buds of wild-type and *PRP8Aa;bb* plants before anther dehiscence were emasculated and let mature for 48 h until the stigma papillae fully developed. Pistils were then pollinated with pollen expressing the LAT52pro-GUS construct, pollen grains derived from *PRP8Aa;bb* plants or control wild-type pollen grains. Pistils were collected at 18-20 HAP. Fertilized pistils were dissected under the binocular dissection microscope (Leica) and strings of ovules attached to septum were transferred to GUS staining solution (0.2 M $Na_2HPO_4$, 0.2 M $NaH_2PO_4$, 10 mM EDTA, 0.1% Triton X-100, 1 mM $K_3Fe(CN)_6$, 2 mM X-Gluc). Samples were stained for between 2-48 h. Stained tissues were cleared of chlorophyll by bleaching in ethanol series of 90%, 70%, 50% and 0% (v/v) prior to imaging. Stained pistils were observed under the Nikon TE-2000 microscope equipped with DIC optics for the presence of a blue dot or with Zeiss binoculars containing a CCD camera for overall pollen tube growth through the pistil.

### Pollen tube cultivation

*In vitro* pollen tube growth was performed according to the protocol of Boavida and McCormick (2007). Pollen tube length was measured after 8 h of *in vitro* growth using the NIS Elements software. For semi-*in vivo* pollen tube growth assay, sterile *ms1* pistils were pollinated with wild-type or *PRP8Aa;bb* pollen and pistils were collected at 1-2 HAP. Pistils were excised at the stigma shoulder with a needle and transferred to the growth medium (Palanivelu et al., 2006) on a small Petri dish. Pistils were tilted to enable the pollen tubes to emerge onto the solid medium surface and cultivated in a humidified growth chamber at 22°C for 24 h. Pollen tube length was measured using the NIS Elements software from the point where they emerged from the cut pistil.

### Statistics

All statistical analysis was performed using Welch's analysis of unequal variances, Chi square test and Student's *t*-test where appropriate.

### RNA extraction and qRT-PCR analysis

Tissue samples were collected and frozen in liquid nitrogen. RNA was extracted using RNeasy Plant Mini Kit (Qiagen) and treated with RQ1 RNAse-free DNase I (Promega). First strand cDNA synthesis was conducted using recombinant M-MLV reverse transcriptase (Promega). qRT-PCR measurements were obtained using LightCycler 480 Instrument (Roche). Relative expression quantification was obtained using the ΔΔCT method following the manufacturer's instructions. Oligonucleotides were designed to distinguish between *Arabidopsis PRP8A* and *PRP8B* genes. Specificity of the oligonucleotides was verified by sequencing of purified PCR products. All measurements were conducted in three biological and two technical replicates.

### Sequences, alignment and phylogenetic analysis

Protein sequences of AtPRP8A and its homologs were downloaded from Phytozome v12.1 (www.phytozome.jgi.doe.gov) and NCBI (https://www.ncbi.nlm.nih.gov) databases. Multiple sequence alignment was carried out using T-Coffee algorithm (Notredame et al., 2000) or Clustal Omega and processed in Jalview alignment editor (Waterhouse et al., 2009). The phylogenetic tree shown in Fig. 1A was constructed using PhyML software (Guindon et al., 2010). Numbers at the nodes of the phylogenetic tree correspond to approximate likelihood ratio test with SH-like (Shimodaira–Hagesawa-like) support from maximum likelihood method. The phylogenetic tree was visualized and processed in Mega 6 software (Tamura et al., 2013). If multiple copies of PRP8 were present in one organism, they were labeled as 'a' or 'b' variants. Variants 'a' were sequentially more similar to AtPRP8A. This labeling does not reflect the phylogenetic relationship between homologs from different organisms.

#### Acknowledgements

We thank Daisuke Kurihara (Nagoya University), Gerd Jürgens (Max Planck Institute for Developmental Biology, Tübingen), Stefanie Sprunck (University of Regensburg), Mark Johnson (Brown University) and Rita Gross-Hardt (University of Bremen) for cell fate markers. We thank Christos Michaelidis and Kamil Růžička, (IEB ASCR, Prague), Ivan Kulich (University of Regensburg) and Roman Pleskot (Ghent University) for valuable discussion, and Zuzana Gadiou and Jana Fecikova for technical assistance. We acknowledge the Imaging Facility of the Institute of Experimental Botany CAS, which is supported by the MEYS CR (LM2018129

Czech-BioImaging and OPPK CZ.2.16/3.1.00/21519 projects), for providing microscope facilities; the SALK Institute for providing the sequence-indexed *Arabidopsis* T-DNA insertion lines and the Nottingham Arabidopsis Stock Centre for providing the lines.

### Competing interests
The authors declare no competing or financial interests.

### Author contributions
Conceptualization: S.S.H., D.H.; Methodology: S.S.H., K.K., V.K., L.S., B.K., L.T., M.J.; Software: S.S.H., B.K., M.J.; Validation: S.S.H., K.K.; Formal analysis: S.S.H., K.K., V.K., M.J.; Investigation: S.S.H., K.K., V.K.; Resources: S.S.H., L.S.; Data curation: S.S.H., K.K., V.K., B.K.; Writing - original draft: S.S.H.; Writing - review & editing: S.S.H., L.T., D.H.; Visualization: S.S.H., K.K., L.S., L.T.; Supervision: S.S.H.; Project administration: S.S.H.; Funding acquisition: S.S.H.

### Funding
This work was financed by the Grantová agentura České republiky (17-23203S, 18-02448S and 19-01723S) and by the Ministerstvo školství, mládeže a tělovýchovy České republiky (LTAUSA18115). The work was also supported by a European Regional Development Fund project 'Centre for Experimental Plant Biology' (CZ.02.1.01/0.0/0.0/16_019/0000738). We also acknowledge Prague Structural Funds (CZ.2.16/3.1.00/21519).

### Data availability
RNA-seq data have been deposited in GEO under accession number GSE151462.

### Supplementary information
Supplementary information available online at
http://dev.biologists.org/lookup/doi/10.1242/dev.186742.supplemental

### References
**Alandete-Saez, M., Ron, M. and McCormick, S.** (2008). GEX3, expressed in the male gametophyte and in the egg cell of Arabidopsis thaliana is essential for micropylar pollen tube guidance and plays a role during early embryogenesis. *Mol. Plant* **1**, 586-598. doi:10.1093/mp/ssn015

**Anders, S., Reyes, A. and Huber, W.** (2012). Detecting differential usage of exons from RNA-seq data. *Genome Res.* **22**, 2008-2017. doi:10.1101/gr.133744.111

**Bartels, C., Klatt, C., Lührmann, R. and Fabrizio, P.** (2002). The ribosomal translocase homologue Snu114p is involved in unwinding U4/U6 RNA during activation of the spliceosome. *EMBO Rep.* **3**, 875-880. doi:10.1093/embo-reports/kvf172

**Bayer, M., Nawy, T., Giglione, C., Galli, M., Meinnel, T. and Lukowitz, W.** (2009). Paternal control of embryonic patterning in Arabidopsis thaliana. *Science* **323**, 1485-1488. doi:10.1126/science.1167784

**Beale, K. M., Leydon, A. R. and Johnson, M. A.** (2012). Gamete fusion is required to block multiple pollen tubes from entering an Arabidopsis ovule. *Curr. Biol.* **22**, 1090-1094. doi:10.1016/j.cub.2012.04.041

**Belmonte, M. F., Kirkbride, R. C., Stone, S. L., Pelletier, J. M., Bui, A. Q., Yeung, E. C., Hashimoto, M., Fei, J., Harada, C. M., Munoz, M. D. et al.** (2013). Comprehensive developmental profiles of gene activity in regions and subregions of the Arabidopsis seed. *Proc. Natl. Acad. Sci. USA* **110**, E435-E444. doi:10.1073/pnas.1222061110

**Benjamini, Y. and Hochberg, Y.** (1990). Controlling the false discovery rate: a practical and powerful approach to multiple testing. *J. R. Stat. Soc.* **57**, 289-300. doi:10.1111/j.2517-6161.1995.tb02031.x

**Berget, S. M., Moore, C. and Sharp, P. A.** (1977). Spliced segments at the 5′ terminus of adenovirus 2 late mRNA. *Proc. Natl. Acad. Sci. USA* **74**, 3171-3175. doi:10.1073/pnas.74.8.3171

**Boavida, L. C. and McCormick, S.** (2007). TECHNICAL ADVANCE: temperature as a determinant factor for increased and reproducible in vitro pollen germination in Arabidopsis thaliana. *Plant J.* **52**, 570-582. doi:10.1111/j.1365-313X.2007.03248.x

**Bolger, A. M., Lohse, M. and Usadel, B.** (2014). Trimmomatic: a flexible trimmer for Illumina sequence data. *Bioinformatics* **30**, 2114-2120. doi:10.1093/bioinformatics/btu170

**Borges, F., Gomes, G., Gardner, R., Moreno, N., McCormick, S., Feijó, J. A. and Becker, J. D.** (2008). Comparative transcriptomics of Arabidopsis sperm cells. *Plant Physiol.* **148**, 1168-1181. doi:10.1104/pp.108.125229

**Chaiwongsar, S., Strohm, A. K., Su, S.-H. and Krysan, P. J.** (2012). Genetic analysis of the Arabidopsis protein kinases MAP3Kε1 and MAP3Kε2 indicates roles in cell expansion and embryo development. *Front. Plant Sci.* **3**, 228. doi:10.3389/fpls.2012.00228

**Chen, Y.-H., Li, H.-J., Shi, D.-Q., Yuan, L., Liu, J., Sreenivasan, R., Baskar, R., Grossniklaus, U. and Yang, W.-C.** (2007). The central cell plays a critical role in pollen tube guidance in Arabidopsis. *Plant Cell* **19**, 3563-3577. doi:10.1105/tpc.107.053967

**Christensen, C. A., King, E. J., Jordan, J. R. and Drews, G. N.** (1997). Megagametogenesis in Arabidopsis wild type and the Gf mutant. *Sex. Plant Reprod.* **10**, 49-64. doi:10.1007/s004970050067

**Clough, S. J. and Bent, A. F.** (1998). Floral dip: a simplified method for Agrobacterium-mediated transformation of Arabidopsis thaliana. *Plant J.* **16**, 735-743. doi:10.1046/j.1365-313x.1998.00343.x

**Coury, D. A., Zhang, C., Ko, A., Skaggs, M. I., Christensen, C. A., Drews, G. N., Feldmann, K. A. and Yadegari, R.** (2007). Segregation distortion in Arabidopsis gametophytic factor 1 (gfa1) mutants is caused by a deficiency of an essential RNA splicing factor. *Sex. Plant Reprod.* **20**, 87-97. doi:10.1007/s00497-007-0046-8

**Cui, Z., Tong, A., Huo, Y., Yan, Z., Yang, W., Yang, X. and Wang, X.-X.** (2017). SKIP controls flowering time via the alternative splicing of SEF pre-mRNA in Arabidopsis. *BMC Biol.* **15**, 80. doi:10.1186/s12915-017-0422-2

**Davis, T. C., Jones, D. S., Dino, A. J., Cejda, N. I., Yuan, J., Willoughby, A. C. and Kessler, S. A.** (2017). Arabidopsis thaliana MLO genes are expressed in discrete domains during reproductive development. *Plant Reprod.* **30**, 185-195. doi:10.1007/s00497-017-0313-2

**Deng, X., Lu, T., Wang, L., Gu, L., Sun, J., Kong, X., Liu, C. and Cao, X.** (2016). Recruitment of the NineTeen Complex to the activated spliceosome requires AtPRMT5. *Proc. Natl. Acad. Sci. USA* **113**, 5447-5452. doi:10.1073/pnas.1522458113

**Dobin, A., Davis, C. A., Schlesinger, F., Drenkow, J., Zaleski, C., Jha, S., Batut, P., Chaisson, M. and Gingeras, T. R.** (2013). STAR: ultrafast universal RNA-seq aligner. *Bioinformatics* **29**, 15-21. doi:10.1093/bioinformatics/bts635

**Dresselhaus, T. and Franklin-Tong, N.** (2013). Male-female crosstalk during pollen germination, tube growth and guidance, and double fertilization. *Mol. Plant* **6**, 1018-1036. doi:10.1093/mp/sst061

**Dresselhaus, T., Sprunck, S. and Wessel, G. M.** (2016). Fertilization mechanisms in flowering plants. *Curr. Biol.* **26**, R125-R139. doi:10.1016/j.cub.2015.12.032

**Filichkin, S., Priest, H. D., Megraw, M. and Mockler, T. C.** (2015). Alternative splicing in plants: directing traffic at the crossroads of adaptation and environmental stress. *Curr. Opin. Plant Biol.* **24**, 125-135. doi:10.1016/j.pbi.2015.02.008

**Ge, Z., Bergonci, T., Zhao, Y., Zou, Y., Du, S., Liu, M.-C., Luo, X., Ruan, H., García-Valencia, L. E., Zhong, S. et al.** (2017). *Arabidopsis* pollen tube integrity and sperm release are regulated by RALF-mediated signaling. *Science* **358**, 1596-1600. doi:10.1126/science.aao3642

**Grefen, C. and Blatt, M. R.** (2012). A 2in1 cloning system enables ratiometric bimolecular fluorescence complementation (rBiFC). *BioTechniques* **53**, 311-314. doi:10.2144/000113941

**Gross-Hardt, R., Kägi, C., Baumann, N., Moore, J. M., Baskar, R., Gagliano, W. B., Jürgens, G. and Grossniklaus, U.** (2007). LACHESIS restricts gametic cell fate in the female gametophyte of Arabidopsis. *PLoS Biol.* **5**, e47. doi:10.1371/journal.pbio.0050047

**Guilgur, L. G., Prudêncio, P., Sobral, D., Liszekova, D., Rosa, A. and Martinho, R. G.** (2014). Requirement for highly efficient pre-mRNA splicing during Drosophila early embryonic development. *eLife* **3**, e02181. doi:10.7554/eLife.02181

**Guindon, S., Dufayard, J.-F., Lefort, V., Anisimova, M., Hordijk, W. and Gascuel, O.** (2010). New algorithms and methods to estimate maximum-likelihood phylogenies: assessing the performance of PhyML 3.0. *Syst. Biol.* **59**, 307-321. doi:10.1093/sysbio/syq010

**Hafidh, S., Fíla, J. and Honys, D.** (2016a). Male gametophyte development and function in angiosperms: a general concept. *Plant Reprod.* **29**, 31-51. doi:10.1007/s00497-015-0272-4

**Hafidh, S., Potěšil, D., Fíla, J., apková, V., Zdráhal, Z. and Honys, D.** (2016b). Quantitative proteomics of the tobacco pollen tube secretome identifies novel pollen tube guidance proteins important for fertilization. *Genome Biol.* **17**, 81. doi:10.1186/s13059-016-0928-x

**Hafidh, S., Potěšil, D., Müller, K., Fíla, J., Michailidis, C., Herrmannová, A., Feciková, J., Ischebeck,T., Valášek, L. S., Zdráhal, Z. et al.** (2018). Dynamics of the pollen sequestrome defined by subcellular coupled omics. *Plant Physiol.* **178**, 258-282. doi:10.1104/pp.18.00648

**Higashiyama, T. and Yang, W.** (2017). Gametophytic pollen tube guidance: attractant peptides, gametic controls, and receptors. *Plant Physiol.* **173**, 112-121. doi:10.1104/pp.16.01571

**Honys, D. and Twell, D.** (2004). Transcriptome analysis of haploid male gametophyte development in Arabidopsis. *Genome Biol.* **5**, R85. doi:10.1186/gb-2004-5-11-r85

**Kalyna, M., Simpson, C. G., Syed, N. H., Lewandowska, D., Marquez, Y., Kusenda, B., Marshall, J., Fuller, J., Cardle, L., McNicol, J. et al.** (2012). Alternative splicing and nonsense-mediated decay modulate expression of important regulatory genes in Arabidopsis. *Nucleic Acids Res.* **40**, 2454-2469. doi:10.1093/nar/gkr932

**Kanemori, Y., Koga, Y., Sudo, M., Kang, W., Kashiwabara, S., Ikawa, M., Hasuwa, H., Nagashima, K., Ishikawa, Y., Ogonuki, N. et al.** (2016). Biogenesis of sperm acrosome is regulated by pre-mRNA alternative splicing of Acrbp in the mouse. *Proc. Natl. Acad. Sci. USA* **113**, E3696-E3705. doi:10.1073/pnas.1522333113

**Karimi, M., Inzé, D. and Depicker, A.** (2002). GATEWAY™ vectors for Agrobacterium-mediated plant transformation. *Trends Plant Sci.* **7**, 193-195. doi:10.1016/S1360-1385(02)02251-3

**Kasahara, R. D., Portereiko, M. F., Sandaklie-Nikolova, L., Rabiger, D. S. and Drews, G. N.** (2005). MYB98 is required for pollen tube guidance and synergid cell differentiation in Arabidopsis. *Plant Cell* **17**, 2981-2992. doi:10.1105/tpc.105.034603

**Kim, Y.-E., Park, C., Kim, K. E. and Kim, K. K.** (2018). Histone and RNA-binding protein interaction creates crosstalk network for regulation of alternative splicing. *Biochem. Biophys. Res. Commun.* **499**, 30-36. doi:10.1016/j.bbrc.2018.03.101

**Leydon, A. R., Weinreb, C., Venable, E., Reinders, A., Ward, J. M. and Johnson, M. A.** (2017). The molecular dialog between flowering plant reproductive partners defined by SNP-informed RNA-sequencing. *Plant Cell* **29**. 984-1006. doi:10.1105/tpc.16.00816

**Li, H.-J., Xue, Y., Jia, D.-J., Wang, T., Hi, D.-Q., Liu, J., Cui, F., Xie, Q., Ye, D. and Yang, W.-C.** (2011). POD1 regulates pollen tube guidance in response to micropylar female signaling and acts in early embryo patterning in Arabidopsis. *Plant Cell* **23**, 3288-3302. doi:10.1105/tpc.111.088914

**Li, H.-J., Zhu, S.-S., Zhang, M.-X., Wang, T., Liang, L., Xue, Y., Shi, D.-Q., Liu, J. and Yang, W.-C.** (2015). Arabidopsis CBP1 is a novel regulator of transcription initiation in central cell-mediated pollen tube guidance. *Plant Cell* **27**, 2880-2893. doi:10.1105/tpc.15.00370

**Liao, Y., Smyth, G. K. and Shi, W.** (2014). featureCounts: an efficient general purpose program for assigning sequence reads to genomic features. *Bioinformatics* **30**, 923-930. doi:10.1093/bioinformatics/btt656

**Liu, M., Yuan, L., Liu, N.-Y., Shi, D.-Q., Liu, J. and Yang, W.-C.** (2009). GAMETOPHYTIC FACTOR 1, involved in Pre-mRNA splicing, is essential for megagametogenesis and embryogenesis in arabidopsis. *J. Integr. Plant Biol.* **51**, 261-271. doi:10.1111/j.1744-7909.2008.00783.x

**Liu, Y., Joly, V., Dorion, S., Rivoal, J. and Matton, D. P.** (2015). The plant ovule secretome: a different view toward pollen-pistil interactions. *J. Proteome Res.* **14**, 4763-4775. doi:10.1021/acs.jproteome.5b00618

**Liu, X., Castro, C., Wang, Y., Noble, J., Ponvert, N., Bundy, M., Hoel, C., Shpak, E. and Palanivelu, R.** (2016). The role of LORELEI in pollen tube reception at the interface of the synergid cell and pollen tube requires the modified eight-cysteine motif and the receptor-like kinase FERONIA. *Plant Cell* **28**, 1035-1052. doi:10.1105/tpc.15.00703

**Loraine, A. E., McCormick, S., Estrada, A., Patel, K. and Qin, P.** (2013). RNA-seq of Arabidopsis pollen uncovers novel transcription and alternative splicing. *Plant Physiol.* **162**, 1092-1109. doi:10.1104/pp.112.211441

**Love, M. I., Huber, W. and Anders, S.** (2014). Moderated estimation of fold change and dispersion for RNA-seq data with DESeq2. *Genome Biol.* **15**, 550. doi:10.1186/s13059-014-0550-8

**Luco, R. F., Pan, Q., Tominaga, K., Blencowe, B. J., Pereira-Smith, O. M. and Misteli, T.** (2010). Regulation of alternative splicing by histone modifications. *Science* **327**, 996-1000. doi:10.1126/science.1184208

**Luco, R. F., Allo, M., Schor, I. E., Kornblihtt, A. R. and Misteli, T.** (2011). Epigenetics in alternative pre-mRNA splicing. *Cell* **144**, 16-26. doi:10.1016/j.cell.2010.11.056

**Maeder, C., Kutach, A. K. and Guthrie, C.** (2009). ATP-dependent unwinding of U4/U6 snRNAs by the Brr2 helicase requires the C terminus of PRP8. *Nat. Struct. Mol. Biol.* **16**, 42-48. doi:10.1038/nsmb.1535

**Marquardt, S., Raitskin, O., Wu, Z., Liu, F., Sun, Q. and Dean, C.** (2014). Functional consequences of splicing of the antisense transcript COOLAIR on FLC transcription. *Mol. Cell* **54**, 156-165. doi:10.1016/j.molcel.2014.03.026

**Marquez, Y., Brown, J. W. S., Simpson, C., Barta, A. and Kalyna, M.** (2012). Transcriptome survey reveals increased complexity of the alternative splicing landscape in Arabidopsis. *Genome Res.* **22**, 1184-1195. doi:10.1101/gr.134106.111

**Márton, M. L., Cordts, S., Broadhvest, J. and Dresselhaus, T.** (2005). Micropylar pollen tube guidance by egg apparatus 1 of maize. *Science* **307**, 573-576. doi:10.1126/science.1104954

**Márton, M. L., Fastner, A., Uebler, S. and Dresselhaus, T.** (2012). Overcoming hybridization barriers by the secretion of the maize pollen tube attractant ZmEA1 from Arabidopsis ovules. *Curr. Biol.* **22**, 1194-1198. doi:10.1016/j.cub.2012.04.061

**McGlincy, N. J. and Smith, C. W. J.** (2008). Alternative splicing resulting in nonsense-mediated mRNA decay: what is the meaning of nonsense? *Trends Biochem. Sci.* **33**, 385-393. doi:10.1016/j.tibs.2008.06.001

**Mecchia, M. A., Santos-Fernandez, G., Duss, N. N., Somoza, S. C., Boisson-Dernier, A., Gagliardini, V., Martínez-Bernardini, A., Fabrice, T. N., Ringli, C., Muschietti, J. P. et al.** (2017). RALF4/19 peptides interact with LRX proteins to control pollen tube growth in Arabidopsis. *Science* **358**, 1600-1603. doi:10.1126/science.aao5467

**Meinke, D., Muralla, R., Sweeney, C. and Dickerman, A.** (2008). Identifying essential genes in Arabidopsis thaliana. *Trends Plant Sci.* **13**, 483-491. doi:10.1016/j.tplants.2008.06.003

**Middleton, R., Gao, D., Thomas, A., Singh, B., Au, A., Wong, J. J.-L., Bomane, A., Cosson, B., Eyras, E., Rasko, J. E. et al.** (2017). IRFinder: assessing the impact of intron retention on mammalian gene expression. *Genome Biol.* **18**, 51. doi:10.1186/s13059-017-1184-4

**Mithoe, S. C., Ludwig, C., Pel, M. J. C., Cucinotta, M., Casartelli, A., Mbengue, M., Sklenar, J., Derbyshire, P., Robatzek, S., Pieterse, C. M. J. et al.** (2016). Attenuation of pattern recognition receptor signaling is mediated by a MAP kinase kinase kinase. *EMBO Rep.* **17**, 441-454. doi:10.15252/embr.201540806

**Moll, C., Von Lyncker, L., Zimmermann, S., Kägi, C., Baumann, N., Twell, D., Grossniklaus, U. and Groß-Hardt, R.** (2008). CLO/GFA1 and ATO are novel regulators of gametic cell fate in plants. *Plant J.* **56**, 913-921. doi:10.1111/j.1365-313X.2008.03650.x

**Mori, T., Kuroiwa, H., Higashiyama, T. and Kuroiwa, T.** (2006). GENERATIVE CELL SPECIFIC 1 is essential for angiosperm fertilization. *Nat. Cell Biol.* **8**, 64-71. doi:10.1038/ncb1345

**Muschietti, J., Dircks, L., Vancanneyt, G. and McCormick, S.** (1994). LAT52 protein is essential for tomato pollen development: pollen expressing antisense LAT52 RNA hydrates and germinates abnormally and cannot achieve fertilization. *Plant J.* **6**, 321-338. doi:10.1046/j.1365-313X.1994.06030321.x

**Notredame, C., Higgins, D. G. and Heringa, J.** (2000). T-coffee: a novel method for fast and accurate multiple sequence alignment. *J. Mol. Biol.* **302**, 205-217. doi:10.1006/jmbi.2000.4042

**Okuda, S., Tsutsui, H., Shiina, K., Sprunck, S., Takeuchi, H., Yui, R., Kasahara, R. D., Hamamura, Y., Mizukami, A., Susaki, D. et al.** (2009). Defensin-like polypeptide LUREs are pollen tube attractants secreted from synergid cells. *Nature* **458**, 357-361. doi:10.1038/nature07882

**Pagnussat, G. C., Yu, H. J., Ngo, Q. A., Rajani, S., Mayalagu, S., Johnson, C. S., Capron, A., Xie, L. F., Ye, D. and Sundaresan, V.** (2005). Genetic and molecular identification of genes required for female gametophyte development and function in Arabidopsis. *Development* **132**, 603-614. doi:10.1242/dev.01595

**Palanivelu, R., Preuss, D., Weterings, K., Russell, S., Lord, E., Russell, S., Huck, N., Moore, J., Federer, M., Grossniklaus, U. et al.** (2006). Distinct short-range ovule signals attract or repel Arabidopsis thaliana pollen tubes in vitro. *BMC Plant Biol.* **6**, 7. doi:10.1186/1471-2229-6-7

**Qin, Y., Leydon, A. R., Manziello, A., Pandey, R., Mount, D., Denic, S., Vasic, B., Johnson, M. A. and Palanivelu, R.** (2009). Penetration of the stigma and style elicits a novel transcriptome in pollen tubes, pointing to genes critical for growth in a pistil. *PLoS Genet.* **5**, e1000621. doi:10.1371/journal.pgen.1000621

**Reddy, A. SN., Marquez, Y., Kalyna, M. and Barta, A.** (2013). Complexity of the alternative splicing landscape in plants. *Plant Cell* **25**, 3657-3683. doi:10.1105/tpc.113.117523

**Robinson, M. D., McCarthy, D. J. and Smyth, G. K.** (2010). edgeR: a Bioconductor package for differential expression analysis of digital gene expression data. *Bioinformatics* **26**, 139-140. doi:10.1093/bioinformatics/btp616

**Schwartz, B. W., Yeung, E. C. and Meinke, D. W.** (1994). Disruption of morphogenesis and transformation of the suspensor in abnormal suspensor mutants of Arabidopsis. *Development* **120**, 3235-3245.

**Shimizu, K. K., Ito, T., Ishiguro, S. and Okada, K.** (2008). MAA3 (MAGATAMA3) helicase gene is required for female gametophyte development and pollen tube guidance in Arabidopsis thaliana. *Plant Cell Physiol.* **49**, 1478-1483. doi:10.1093/pcp/pcn130

**Staiger, D. and Brown, J. W. S.** (2013). Alternative splicing at the intersection of biological timing, development, and stress responses. *Plant Cell* **25**, 3640-3656. doi:10.1105/tpc.113.113803

**Syed, N. H., Kalyna, M., Marquez, Y., Barta, A. and Brown, J. W. S.** (2012). Alternative splicing in plants: coming of age. *Trends Plant Sci.* **17**, 616-623. doi:10.1016/j.tplants.2012.06.001

**Takeuchi, H. and Higashiyama, T.** (2012). A species-specific cluster of defensin-like genes encodes diffusible pollen tube attractants in Arabidopsis. *PLoS Biol.* **10**, e1001449. doi:10.1371/journal.pbio.1001449

**Tamura, K., Stecher, G., Peterson, D., Filipski, A. and Kumar, S.** (2013). MEGA6: molecular evolutionary genetics analysis version 6.0. *Mol. Biol. Evol.* **30**, 2725-2729. doi:10.1093/molbev/mst197

**Tang, W., Ezcurra, I., Muschietti, J. and McCormick, S.** (2002). A cysteine-rich extracellular protein, LAT52, interacts with the extracellular domain of the pollen receptor kinase LePRK2. *Plant Cell* **14**, 2277-2287. doi:10.1105/tpc.003103

**Tresini, M., Warmerdam, D. O., Kolovos, P., Snijder, L., Vrouwe, M. G., Demmers, J. AA., van IJcken, W. FJ., Grosveld, F. G., Medema, R. H., Hoeijmakers, J. HJ. et al.** (2015). The core spliceosome as target and effector of non-canonical ATM signalling. *Nature* **523**, 53-58. doi:10.1038/nature14512

**Twell, D., Yamaguchi, J. and McCormick, S.** (1990). Pollen specific gene expression in transgenic plants: coordinate regulation of two different tomato gene promoters during microsporogenesis. *Development* **109**, 705-713.

**Twell, D., Yamaguchi, J., Wing, R. A., Ushiba, J. and McCormick, S.** (1991). Promoter analysis of genes that are coordinately expressed during pollen development reveals pollen-specific enhancer sequences and shared regulatory elements. *Genes Dev.* **5**, 496-507. doi:10.1101/gad.5.3.496

**Tzafrir, I., Pena-muralla, R., Dickerman, A., Berg, M., Rogers, R., Hutchens, S., Sweeney, T. C., Mcelver, J., Aux, G., Patton, D. et al.** (2004). Identification of genes required for embryo development in arabidopsis. *Plant Physiol.* **135**, 1206-1220. doi:10.1104/pp.104.045179

**Völz, R., Heydlauff, J., Ripper, D., von Lyncker, L. and Groß-Hardt, R.** (2013). Ethylene signaling is required for synergid degeneration and the establishment of a pollen tube block. *Dev. Cell* **25**, 310-316. doi:10.1016/j.devcel.2013.04.001

**von Besser, K., Frank, A. C., Johnson, M. A. and Preuss, D.** (2006). Arabidopsis HAP2 (GCS1) is a sperm-specific gene required for pollen tube guidance and fertilization. *Development* **133**, 4761-4769. doi:10.1242/dev.02683

**Wang, Y., Tsukamoto, T., Noble, J. A., Liu, X., Mosher, R. A. and Palanivelu, R.** (2017). Arabidopsis LORELEI, a maternally expressed imprinted gene, promotes early seed development. *Plant Physiol.* **175**, 758-773. doi:10.1104/pp.17.00427

**Waterhouse, A. M., Procter, J. B., Martin, D. MA., Clamp, M. and Barton, G. J.** (2009). Jalview Version 2—a multiple sequence alignment editor and analysis workbench. *Bioinformatics* **25**, 1189-1191. doi:10.1093/bioinformatics/btp033

**Will, C. L. and Lührmann, R.** (2011). Spliceosome structure and function. *Cold Spring Harb. Perspect. Biol.* **3**, a003707. doi:10.1101/cshperspect.a003707

**Winter, D., Vinegar, B., Nahal, H., Ammar, R., Wilson, G. V. and Provart, N. J.** (2007). An "Electronic Fluorescent Pictograph" browser for exploring and analyzing large-scale biological data sets. *PLoS ONE* **2**, e718. doi:10.1371/journal.pone.0000718

**Wuest, S. E., Vijverberg, K., Schmidt, A., Weiss, M., Gheyselinck, J., Lohr, M., Wellmer, F., Rahnenführer, J., von Mering, C. and Grossniklaus, U.** (2010). Arabidopsis female gametophyte gene expression map reveals similarities between plant and animal gametes. *Curr. Biol.* **20**, 506-512. doi:10.1016/j.cub.2010.01.051

**Xu, Y., Zhao, W., Olson, S. D., Prabhakara, K. S. and Zhou, X.** (2018). Alternative splicing links histone modifications to stem cell fate decision. *Genome Biol.* **19**, 133. doi:10.1186/s13059-018-1512-3

**Yang, C., Vizcay-Barrena, G., Conner, K. and Wilson, Z. A.** (2007). MALE STERILITY1 is required for tapetal development and pollen wall biosynthesis. *Plant Cell* **19**, 3530-3548. doi:10.1105/tpc.107.054981

**Zhang, X., Yan, C., Hang, J., Finci, L. I., Lei, J. and Shi, Y.** (2017). An Atomic Structure of the Human Spliceosome. *Cell* **169**, 1-12. doi:10.1016/j.cell.2017.04.033

**Zimmermann, P., Hirsch-Hoffmann, M., Hennig, L. and Gruissem, W.** (2004). Genevestigator: arabidopsis microarray database and analysis toolbox. *Plant Biol.* **2004**, 186. doi:10.1104/pp.104.046367